European Journal of Medicinal Chemistry 70 (2013) 723–739

Contents lists available at ScienceDirect

European Journal of Medicinal Chemistry

journal homepage: http://www.elsevier.com/locate/ejmech

Original article

Fine molecular tuning at position 4 of 2*H*-chromen-2-one derivatives in the search of potent and selective monoamine oxidase B inhibitors

Leonardo Pisani [a], Marco Catto [a], Orazio Nicolotti [a], Giancarlo Grossi [b], Mario Di Braccio [b], Ramon Soto-Otero [c], Estefania Mendez-Alvarez [c], Angela Stefanachi [a], Domenico Gadaleta [a], Angelo Carotti [a,*]

[a] *Dipartimento di Farmacia – Scienze del Farmaco, Università degli Studi di Bari "Aldo Moro", via E. Orabona 4, I-70125 Bari, Italy*
[b] *Dipartimento di Scienze Farmaceutiche, Università degli Studi di Genova, viale Benedetto XV 3, I-16132 Genova, Italy*
[c] *Grupo de Neuroquimica, Departamento de Bioquimica y Biologia Molecular, Facultad de Medicina, Universidad de Santiago de Compostela, San Francisco I E-15782, Santiago de Compostela, Spain*

ARTICLE INFO

Article history:
Received 26 June 2013
Received in revised form
11 September 2013
Accepted 14 September 2013
Available online 17 October 2013

Keywords:
Monoamine oxidase inhibitors
4-Substituted-7-benzyloxy-2*H*-chromene-2-ones
Molecular docking
Selective MAO-B inhibitors
Parkinson's disease
Alzheimer's disease
Neurodegenerative diseases

ABSTRACT

The effects on the inhibition potencies of monoamine oxidase isoforms A (MAO-A) and B (MAO-B) depending upon changes in the physicochemical properties (size, shape, H-bonding, lipophilicity, etc.) of substituents at the C4 position of 2*H*-chromen-2-one derivatives were extensively investigated, and the results significantly added to our knowledge on this class of MAO inhibitors. All the 67 examined compounds showed high MAO-B selectivity, some of them achieving potency in the low nanomolar range. In particular, the 7-metachlorobenzyloxy-4-oxyacetamido-2*H*-chromen-2-one (entry 62) showed single digit nanomolar MAO-B potency (IC_{50} = 3.1 nM) and high selectivity over the MAO-A isoform (selectivity ratio = 7244). The great variety of the investigated substituents at C4 of the 2*H*-chromen-2-one nucleus, combined with binding models generated from docking studies carried out on selected compounds, allowed us to shed light on the main molecular requirements for potent and selective MAO-B inhibition, highlighting the dominant role of the steric effects. Interestingly, many of the designed substituents could be metabolically related to each other (e.g., CH_3/CH_2OH/CHO/COOH; NH_2/$NHCH_3$, NHAc), and therefore the results obtained may help in predicting the in vivo activity of some putative metabolites of lead MAO-B inhibitors.

1. Introduction

Monoamine oxidases (MAOs, E.C. 1.4.3.4, amine-oxygen oxidoreductase) are responsible for the catalytic oxidative deamination of endogenous and exogenous arylalkylamines to the corresponding iminium salts that subsequently are non-enzymatically hydrolyzed to the final aldehyde products [1]. The catalytic cycle employs molecular oxygen as the electron acceptor and produces lower molecular weight amines, or ammonia (from primary amines), and the hydrogen peroxide that triggers the formation of reactive oxygen species (ROS) as harmful by-products. Even though over the years detailed studies have been dedicated to MAOs structure and function, the mechanistic features of the oxidative pathway catalyzed by MAOs are still under debate. Different hypotheses have been formulated and, among others, single electron transfer and polar nucleophilic mechanisms appear as the most plausible ones being sustained by more robust experimental evidence [2].

MAO substrates include dietary amines (e.g., tyramine), monoamine neurotransmitters (e.g., serotonin, histamine and catecholamines, such as epinephrine, norepinephrine and dopamine) and the Parkinson-inducing neurotoxin 1-methyl-4-phenyl-1,2,3,6-tetrahydropyridine (MPTP). After the seminal paper describing two different MAO isoforms in 1968, termed MAO-A and -B [3], great research efforts have been devoted to the understanding of their main structural and functional differences, often related to species diversity. Encoded by two different genes on X chromosome, the two isoenzymes show nearly 70% sequence identity and share close biological functions [4]. Flavin adenine dinucleotide (FAD), covalently linked through a thioether bond to a cysteine residue of the MAO protein backbone, serves as redox prosthetic cofactor in the oxidative deamination process. The highly hydrophobic C-terminal α-helix anchors each isoenzymes to the outer

* Corresponding author. Tel.: +39 080 5442782; fax: +39 080 5442230.
E-mail addresses: angelo.carotti@uniba.it, carotti_angelo@hotmail.com (A. Carotti).

0223-5234/$ – see front matter © 2013 Elsevier Masson SAS. All rights reserved.
http://dx.doi.org/10.1016/j.ejmech.2013.09.034

mitochondrial membrane with a characteristic dimeric fashion [5], which made their isolation and purification troublesome. The identification and optimization of efficient high-throughput expression and purification systems [6–8] paved the way for the preparation of protein-inhibitors co-crystals. The X-ray determination at high resolution of MAO complexed with both reversible and irreversible inhibitors enlightened the main molecular determinants governing the binding interactions in the active site and allowed the identification of the key three-dimensional structural differences between the two isoenzymes [9]. The MAO enzymatic active site is a lipophilic cage, largely filled by aromatic amino acids, surrounding the isoalloxazine moiety of the FAD cofactor. The diverse shape and structure of this region in MAO-A and MAO-B result in the different selectivity/affinity for substrates and inhibitors [4]. Depending on the bound substrate/inhibitor, MAO-B active site can exhibit a bipartite cavity so that the ligand has to negotiate a smaller entrance room before entering the substrate cavity where FAD is accommodated. As an alternative, these two subsites may be merged because of conformational changes of a flexible residue (Ile199) occurring upon binding of specific ligands spanning both cavities (e.g., 1,4-diphenyl-2-butene and *trans*,*trans*-farnesol) [10]. This bipartite protein motif is absent in MAO-A, where the "gate-keeper" Ile199 residue is replaced by a Phe208 (numbering are referred to human enzymes) and the substrate/inhibitor has to gain access to a unique and wide hydrophobic pocket containing FAD [11,12].

Most mammalian peripheral tissues express both MAO isoforms, with the exception of platelets which contain just MAO-B [13]. High levels of MAO-A have been found in placenta and intestine. Marked differences in brain distribution have been described in humans through positron emission tomography (PET) experiments [14]. The prevalence of MAO-A in brain areas under catecholamine control (e.g., substantia nigra and locus coeruleus) has been documented. MAO-B has been mainly localized in astrocytes, basal ganglia, dorsal raphe nucleus and blood–brain barrier microvessels [15]. In neurons and glial cells, the catalytic activity of MAOs exerts the function of protecting from exogenous amines and terminating the nerve impulse signalling.

The ability of MAOs to control the levels of neurotransmitters in central nervous system (CNS) attracted the interest of many researchers involved in the discovery of new drugs targeting brain disorders [16,17]. Broad consensus about the clinical relevance of MAO inhibition raised when abnormalities in central MAO-A and -B enzymatic activity have been associated to behavioural disturbances and Parkinson's disease (PD), respectively [18]. Propargylamines (e.g., clorgyline and selegiline), hydrazine derivatives (e.g., phenelzine) and arylcyclopropylamines (e.g., tranylcypromine) have been described as mechanism-based irreversible inhibitors (Chart 1). After initial fitting to MAOs enzymatic site, these inhibitors are transformed into suicide inhibitors, as a consequence of the catalytic activity itself, that inactivate the enzyme by forming covalent bonds to isoalloxazine N(5) or C(4a) atoms [9]. The formation of FAD adducts is allowed by the unusual bent conformation of the tricyclic isoalloxazine skeleton. Aryl oxazolidinones (e.g., toloxatone), brofaromine and moclobemide belong to the class of MAO reversible inhibitors, which can be further classified as competitive or slow, tight-binding inhibitors [19].

Although abundance of MAOs in liver, placenta, intestine and lung [20] exceeds by far brain expression, little is known about their physiological role in non-cerebral districts. Moreover, the activity of MAO inhibitors (MAO-Is) in peripheral tissues has been largely associated with the toxicity of the earliest non-selective and irreversible inhibitors. Hypertensive crises have been ascribed to the potentiation of sympathomimetic amines such as tyramine (mainly present in cheese and red wine and hence triggering the so called "cheese-effect") that is not scavenged by MAOs after inhibitors administration. Hepatotoxic reactions have been related to the inhibition of CYP450s activity. In addition to the above-mentioned, unwanted and severe side-effects, stringent dietary restrictions and harmful drug–drug interactions explain the reasons why some MAO inhibitors have been discontinued in the clinical practice. In order to overcome the toxicity issue, the research on MAO-Is has been focused on solving chiefly the selectivity problem. In this way, moclobemide (a reversible and selective MAO-A inhibitor) [21] and a transdermal formulation system of selegiline [22] (irreversible and selective MAO-B inhibitor) were discovered and marketed

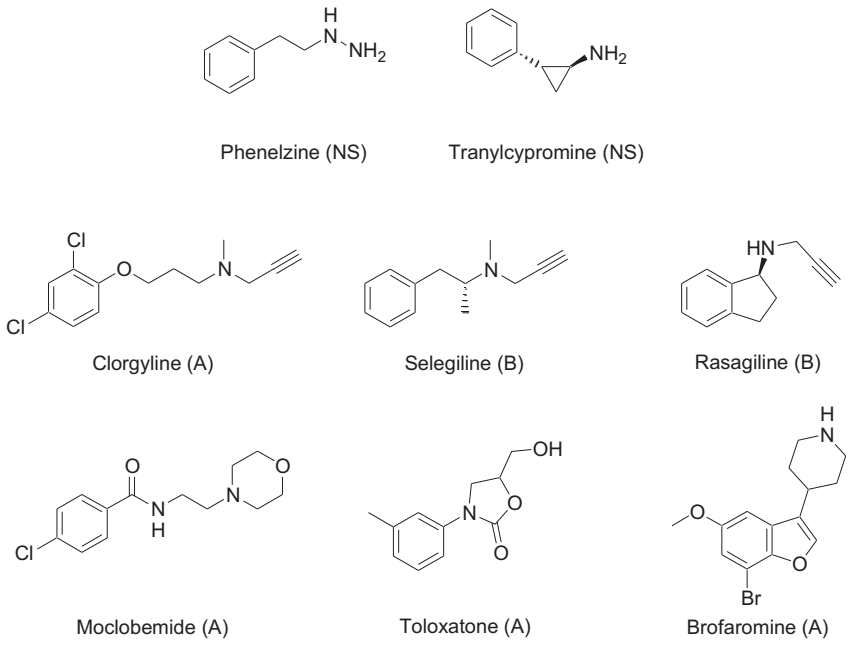

Chart 1. Chemical structures of non-selective and selective reversible and irreversible inhibitors of monoamine oxidases A and B.

against depressive disturbances. On the other side, selective MAO-BIs (e.g., rasagiline) [23] have been adopted in the treatment of PD as dopamine-sparing agents. Recent trials [24] suggested a potential disease-modifying effects of rasagiline in early PD as an alternative to long-term levodopa treatment that is associated to disabling motor impairments (e.g., motor fluctuations and dyskynesia).

Initially conceived as therapeutics to treat depressive disturbances and PD, and after a brief decline linked to the clear-cut unwanted toxic effects, a renewed interest towards MAO inhibitors is flourishing nowadays. Recent studies unravelled a novel role for MAO-A [25] and MAO-B [26] in the pathogenesis and progression of heart failure because of MAO-driven ROS production, enhanced norepinephrine catabolism and impaired aldehyde metabolism. Moreover, enabling the diminishment of ROS production, MAO-Is have been proposed as neuroprotectants against many debilitating neurodegenerative diseases (NDs) linked to ageing and oxidative stress [27]. The multi-factorial nature of these disorders claims for a paradigmatic shift in the drug discovery process that should be mainly oriented to multi-target ligands able to modulate multiple and differently altered biochemical pathways in a synergic manner [28,29]. Multi-potent compounds showing MAO inhibition as the core activity might exhibit high therapeutic potential against multifaceted brain disorders such as Alzheimer's disease (AD), PD, Huntington's disease (HD), and amyotrophic lateral sclerosis (ALS) [30].

Different heterocyclic scaffolds have been explored to design selective and reversible MAO-A/-B inhibitors. Among them, 2*H*-chromene-2-ones, that is coumarins, have been investigated as potent and selective MAO-Is [31] because their well-consolidated chemistry enables an easy access to mono- and poly-substituted derivatives with a great molecular diversity. The most explored position has been position 7 where appropriate substituents may confer to the molecule high affinity and, more so, selectivity towards either one of the two MAO enzymatic isoforms [32]. Interestingly, similar results came from a recent study of benzofuran analogues carrying substituents at position 6 that can be considered as topologically equivalent to position 7 of coumarin [33]. 3-Substituted coumarins have also been studied as moderately to highly potent and selective MAO-B inhibitors, by the groups of Chimenti [34,35] and Uriarte [36,37]. The position 4 has been also explored by considering chiefly hydrophobic [38], and more occasionally, hydrophilic substituents [39]. As substituents at position 4 play a pivotal role in determining a productive binding of coumarin-based MAO-B inhibitors, in the present work a rational and systematic exploitation of physicochemical and spatial domain of that region was carried out with the design, synthesis and biological evaluation of a large series of 2*H*-chromen-2-one derivatives bearing at position 4 mainly polar substituents, including ionized carboxylic, enolic and amino groups. The large variety of inspected substituent/molecular properties allowed the derivation of sound SAR while docking simulations provided easily interpretable binding modes and enabled the detection of the main molecular requirements for potent and selective MAO-B inhibition. In this regard, outstanding in vivo data have been collected in the past for derivative **13f** that can be taken as the reference compound for its potent and selective MAO-B inhibition both in vitro and in vivo [39,40]. The great modulation of lipophilicity, water solubility and metabolic stability of the designed molecules should guarantee a successful inhibitor selection for oral administration and specific delivery and high activity at the CNS. Interestingly, many of the designed substituents/molecules can be seen as metabolically-related and this would prospect a reliable prediction of their pharmacokinetic profile and in vivo activity. Eventually the original insights from the present work will help the design of new, in vivo-active, multitarget-directed ligands having the selective MAO-B inhibition as the core biological activity [30].

2. Chemistry

The synthetic routes to 4-substituted coumarin derivatives **2a**–**d**, **3a**–**p**, **4a**, **5a**, **6a**–**f**, **7**–**9**, **10a**–**d**, **11a**–**d**, **13a**–**n**, **14**–**18** and **20**–**22** are illustrated in Schemes 1–6.

1-(2,4-Dihydroxyphenyl)ethanone was treated with proper benzyl halides to give the corresponding benzyloxyderivatives **1a**–**d** (anhydrous K_2CO_3, dry 2-butanone at reflux) whose cyclocondensation with diethyl carbonate in the presence of Na (Dowtherm A, 160 °C) afforded the sodium salt of 4-hydroxycoumarin derivatives **2a**–**d** [41], from which 4-hydroxycoumarins were obtained by treatment with aqueous hydrochloric acid. 4-Alkoxyderivatives **3a**–**p** were obtained in satisfactory yields by treating the sodium salts of appropriate 4-hydroxycoumarins **2a**–**d**, with proper alkyl halides in DMF at room temperature (Scheme 1).

As shown in Scheme 2, the reaction of 7-substituted-4-hydroxycoumarins **2c**,**d** with ethyl bromoacetate in refluxing 2-butanone in the presence of anhydrous K_2CO_3 afforded ethyl 4-oxyacetates **4a**,**b**, which in turn were transformed into the corresponding acids **5a**,**b** through saponification with KOH in ethanol. The reaction of acids **5a**,**b** with an excess of $SOCl_2$ in refluxing CH_2Cl_2 gave the corresponding acyl chlorides, which were treated with excess 30% aqueous ammonia or with an excess of suitable amines in CH_2Cl_2 solution yielding amides **6a**,**b** or **6c**–**f** (Scheme 2). Dehydration of the 4-oxyacetamide **6b** in refluxing $POCl_3$ afforded the corresponding nitrile **7** (Scheme 2).

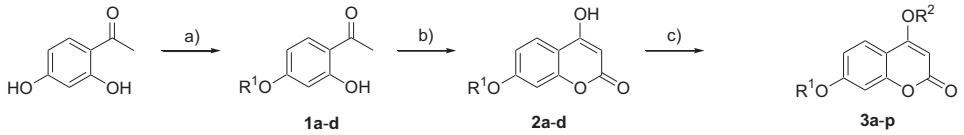

1a, **2a** R^1 = Bn
1b, **2b** R^1 = 3'-FBn
1c, **2c** R^1 = 3'-ClBn
1d, **2d** R^1 = 3'-BrBn

3a	R^1 = Bn; R^2 = CH_3	**3i**	R^1 = 3'-ClBn; R^2 = *n*-C_3H_7
3b	R^1 = Bn; R^2 = C_2H_5	**3j**	R^1 = 3'-BrBn; R^2 = CH_3
3c	R^1 = Bn; R^2 = *n*-C_3H_7	**3k**	R^1 = 3'-BrBn; R^2 = C_2H_5
3d	R^1 = 3'-FBn; R^2 = CH_3	**3l**	R^1 = 3'-BrBn; R^2 = *n*-C_3H_7
3e	R^1 = 3'-FBn; R^2 = C_2H_5	**3m**	R^1 = 3'-ClBn; R^2 = *i*-C_3H_7
3f	R^1 = 3'-FBn; R^2 = *n*-C_3H_7	**3n**	R^1 = 3'-ClBn; R^2 = CH_2OCH_3
3g	R^1 = 3'-ClBn; R^2 = CH_3	**3o**	R^1 = 3'-ClBn; R^2 = CH_2SCH_3
3h	R^1 = 3'-ClBn; R^2 = C_2H_5	**3p**	R^1 = 3'-ClBn; R^2 = CH_2COCH_3

Scheme 1. Synthesis of 4-hydroxy- and 4-alkyloxy-coumarin derivatives **2a**–**d** and **3a**–**p**. Reagents and conditions: a) appropriate benzyl halide, anhydrous K_2CO_3, 2-butanone, reflux, 24 h; b) i): diethyl carbonate, Na, Dowtherm A, 160 °C, 1 h; ii): aq. HCl; c) (from sodium salt of **2a**–**d**) appropriate alkyl halide, dry DMF, room temperature, 1.5 h.

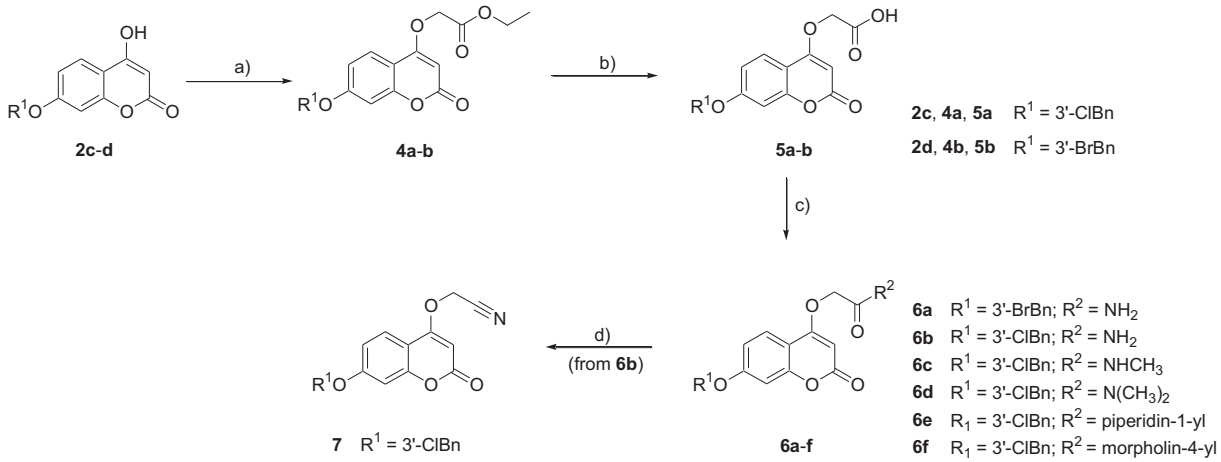

Scheme 2. Synthesis of coumarin derivatives **4a**,**b**, **5a**,**b**, **6a**–**f** and **7**. Reagents and conditions: a) ethyl bromoacetate, anhydrous K_2CO_3, 2-butanone, reflux, 3 h; b) KOH, ethanol, room temperature, 1 h; c) i: $SOCl_2$, CH_2Cl_2, reflux, 2 h; ii: 30% aq. NH_3 or appropriate amine in CH_2Cl_2, room temperature, 30 min; d) from **6b**: $POCl_3$ (excess), reflux, 2 h.

7-[(3-Chlorobenzyl)oxy]-4-hydroxycoumarin **2c** was treated with excess triethylamine in methanol to give a solution of the corresponding triethylammonium salt which, after removal of solvents, was refluxed with excess $POCl_3$ giving 4-chloroderivative **8** (Scheme 3). The reaction of compound **8** with a large excess of phenol afforded the 4-phenoxy derivative **9**. 4-Aminoderivative **10a** was conveniently obtained by the reaction of 4-hydroxyderivative **2c** with excess ammonium acetate in DMSO at 120 °C for 3 h (Scheme 3). The acylation of **10a** in the presence of acetic anhydride under microwave irradiation originated the corresponding amide **10b**. Carbamate derivative **10c** and urea **10d** were obtained by treating **10a** with ethyl chloroformate or ethyl isocyanate, respectively. By reacting 4-chloroderivative **8** with an ethanolic solution of methylamine in a sealed vessel at 60 °C enamine **11a** was obtained. By following the same synthetic strategy, nucleophilic substitutions on 4-chloroderivative **8** with ethylamine hydrochloride (in the presence of triethylamine) or isopropylamine were performed in refluxing CH_2Cl_2 furnishing **11b**,**c**, whereas the synthesis of the anilino derivative **11d** required higher temperature (140 °C), as illustrated in Scheme 3.

4-Substituted-7-hydroxycoumarins **12a** (from commercial source), **12b**,**c** (prepared through a von Pechmann reaction) [39,42] or **12d** [43] underwent benzylation reactions under different conditions with the suitable benzyl bromides affording compounds

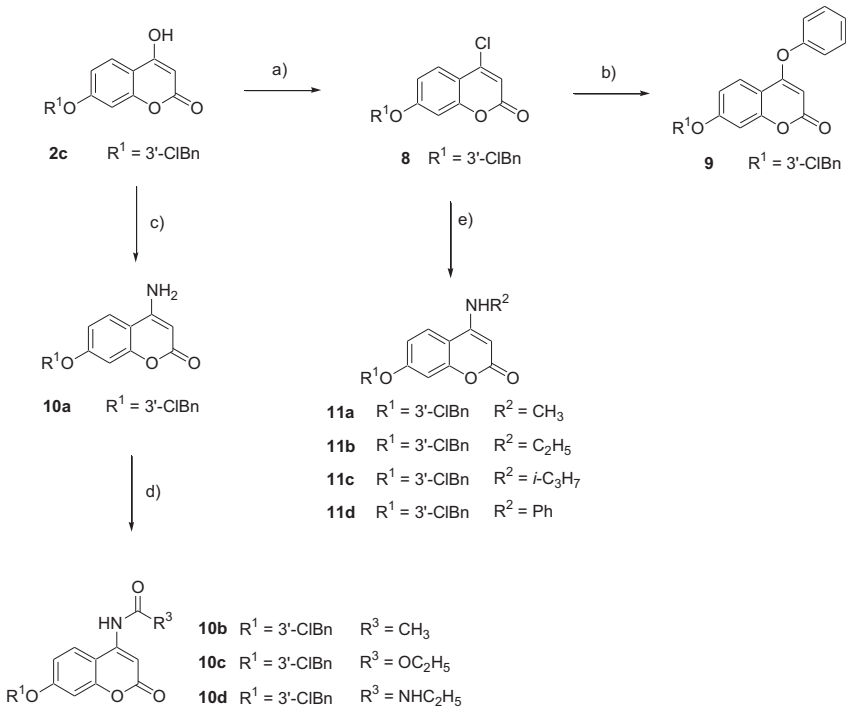

Scheme 3. Synthesis of coumarin derivatives **8**, **9**, **10a**–**d** and **11a**–**d**. Reagents and conditions: a) i): triethylamine, MeOH, room temperature; ii): $POCl_3$, reflux, 3 h; b) phenol, anhydrous K_2CO_3, 2-butanone, reflux, 2 h; c) ammonium acetate, DMSO, 120 °C, 3 h; d) for **10b**: Ac_2O, 150 °C, MW, 30 min; for **10c**: ethyl chloroformate, K_2CO_3, reflux, 10 h; for **10d**: ethyl isocyanate, 60 °C, 120 h; e) for **11a**: methylamine 60% wt. in EtOH, 60 °C, 7 h; for **11b**: ethylamine hydrochloride, triethylamine, EtOH, reflux, 2 h; for **11c**: isopropylamine, CH_2Cl_2, reflux, 5 h; for **11d**: aniline, DIEA, 140 °C, 48 h.

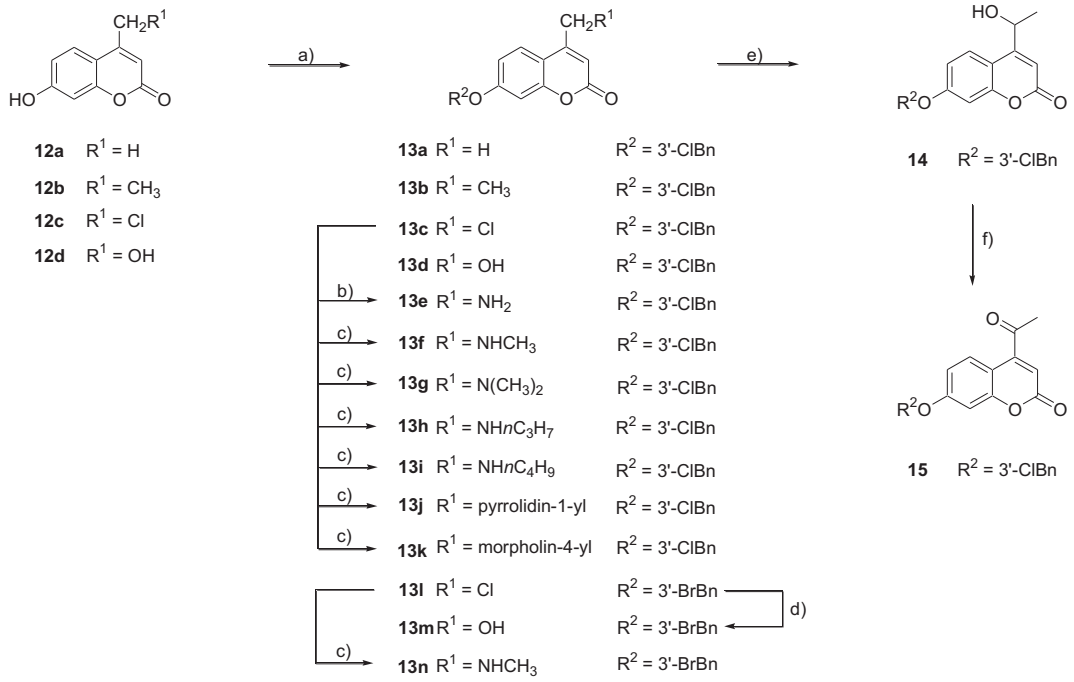

Scheme 4. Synthesis of coumarin derivatives **13a**–**n**, **14** and **15**. Reagents and conditions: a) for **13a**: see Ref. [39]; for **13b**: **12b**, sodium ethoxide, 3′-chlorobenzyl bromide, DMF, 100 °C, 1 h; for **13c,l**: **12c**, Cs_2CO_3, suitable benzyl bromide, DMF, room temperature, 24 h; for **13d**: **12d**, Cs_2CO_3, 3′-chlorobenzyl bromide, DMF, room temperature, 48 h; b) see Ref. [39]: i) sodium azide, EtOH, reflux, 2 h; ii) $SnCl_2$, MeOH, room temperature, 3 h; c) appropriate amine, THF, room temperature, 3 h; d) water, reflux, 48 h; e) from **13b**: SeO_2, xylene, 140 °C, 4 h; f) PCC, dry CH_2Cl_2, room temperature, 2 h.

13a–**c** and **13l** (Scheme 4). Aqueous hydrolysis of chloride **13l** yielded the primary alcohol **13m**. Chlorides **13c** and **13l** were reacted with suitable amines in THF yielding compounds **13e**–**k** and **13n**. The oxidation of the 4-ethylderivative **13b** with SeO_2 in refluxing xylene afforded in moderate yield (43%) 7-[(3-chlorobenzyl)oxy]-4-(1-hydroxyethyl)-2*H*-1-benzopyran-2-one **14**. PCC-mediated oxidation of alcohol **14** afforded ketone **15** (Scheme 4). In the same way, aldehyde **16** was obtained starting from primary alcohol **13d**, as shown in Scheme 5. Compound **16** was then converted into the corresponding oxime **17**, by reaction with $NH_2OH{\cdot}HCl$ in the presence of stoichiometric amount of $AcONa{\cdot}3H_2O$. By refluxing oxime **17** in Ac_2O, dehydration to 4-cyanoderivative **18** was performed.

Ethyl ester **20** was obtained through a reaction between 3-chlorobenzyl bromide and phenol **19** [33] in the presence of caesium carbonate (Scheme 6). Ester **20** was in turn hydrolyzed with KOH to carboxylic acid **21** which was then transformed into the intermediate acyl chloride with $SOCl_2$, that reacted with concentrated aq. NH_3 to afford primary amide **22**.

Compounds **23** and **24** were obtained through benzylation of the suitable commercially available 4-substituted-7-hydroxycoumarins as described in the Experimental section.

The synthetic procedures leading to compounds **13a**, **13e**–**g**, and **25**–**28** (corresponding to entries 23–26 in Table 1) have been already reported elsewhere [39].

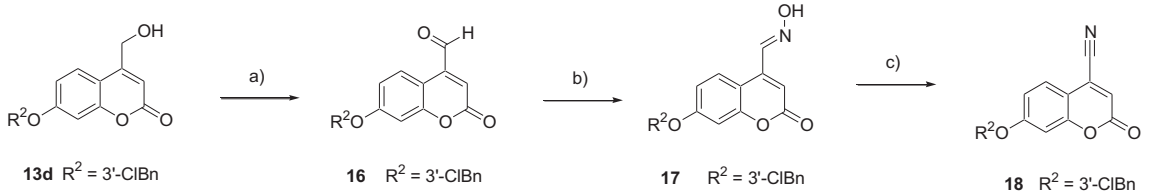

Scheme 5. Synthesis of coumarin derivatives **16**–**18**. Reagents and conditions: a) PCC, sodium acetate, 4 Å mol. sieves, dry CH_2Cl_2, room temperature, 12 h; b) hydroxylamine hydrochloride, sodium acetate, $EtOH/H_2O$, reflux, 30 min; c) Ac_2O, reflux, 15 h.

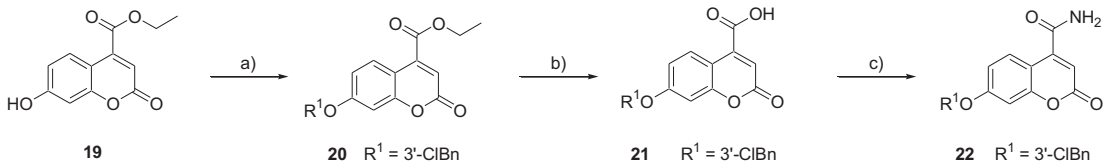

Scheme 6. Synthesis of coumarin derivatives **20**–**22**. Reagents and conditions: a) 3′-chlorobenzyl bromide, Cs_2CO_3, DMF, room temperature, 24 h; b) KOH, ethanol, reflux, 15 min; c) i) $SOCl_2$, CH_2Cl_2, reflux, 2 h; ii) aq. 30% NH_3, room temperature, 6 h.

Table 1
Chemical structure and MAO inhibition data of coumarin derivatives (entries 1–67).

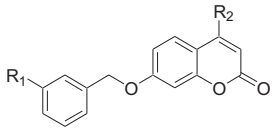

Entry[a]	Compd[b]	R_1	R_2	MAO-A[c]	MAO-B[c]	SI[d]
Class I						
1	**23**	Cl	H	40%	7.77	nd
2	**13a**	Cl	Me	5.28	8.13	2.85
3	**13b**	Cl	Et	48%	7.54	nd
4	**24**	Cl	CF_3	16%	6.06	nd
5	**8**	Cl	Cl	5.05	7.68	2.63
6	**13c**	Cl	CH_2Cl	21%	7.36	nd
7	**13l**	Br	CH_2Cl	28%	6.68	nd
Class II						
8	**2a**	H	OH	2%	5.04	nd
9	**2b**	F	OH	0%	5.68	nd
10	**2c**	Cl	OH	6%	6.32	nd
11	**2d**	Br	OH	0%	6.31	nd
12	**10a**	Cl	NH_2	5.38	7.32	1.94
13	**16**	Cl	CHO	14%	7.28	nd
14	**15**	Cl	$COCH_3$	0%	7.40	nd
15	**21**	Cl	COOH	0%	4.00[e]	nd
16	**20**	Cl	COOEt	4.4%	6.38	nd
17	**22**	Cl	$CONH_2$	14%	6.63	nd
18	**18**	Cl	CN	23%	6.99	nd
19	**17**	Cl	CH=NOH	48%	6.66	nd
Class III						
20	**13d**	Cl	CH_2OH	4.99	8.28	3.29
21	**13m**	Br	CH_2OH	49%	7.85	nd
22	**14**	Cl	$CH(OH)CH_3$	22%	7.11	nd
23	**25**	Cl	CH_2CN	6.33	7.80	1.47
24	**26**	Cl	CH_2CONH_2	4.59	7.52	2.94
25	**27**	Cl	$CH_2CONHMe$	6.30	7.62	1.32
26	**28**	Cl	$CH_2CON(Me)_2$	0%	7.40	nd
27	**13e**	Cl	CH_2NH_2	5.70	7.82	2.12
28	**13f**	Cl	CH_2NHMe	5.23	7.89	2.66
29	**13n**	Br	CH_2NHMe	40%	7.96	nd
30	**13h**	Cl	CH_2NH^nPr	3.2%	6.69	nd
31	**13i**	Cl	CH_2NHnBu	1.1%	6.35	nd
32	**13g**	Cl	$CH_2N(Me)_2$	5.7%	5.95	nd
33	**13j**	Cl	CH_2-1′-pyrrolidinyl	16%	5.77	nd
34	**13k**	Cl	CH_2-4′-morpholinyl	11%	5.64	nd
Class IV						
35	**3a**	H	OMe	22%	7.00	nd
36	**3d**	F	OMe	49%	7.44	nd
37	**3g**	Cl	OMe	4.93	8.11	3.18
38	**3j**	Br	OMe	27%	8.24	nd
39	**3b**	H	OEt	0%	6.12	nd
40	**3e**	F	OEt	25%	6.58	nd
41	**3h**	Cl	OEt	2%	6.94	nd
42	**3k**	Br	OEt	2.5%	6.90	nd
43	**3c**	H	O^nPr	0%	6.24	nd
44	**3f**	F	O^nPr	12%	6.39	nd
45	**3i**	Cl	O^nPr	5.3%	7.21	nd
46	**3l**	Br	O^nPr	0%	7.13	nd
47	**3m**	Cl	O^iPr	3%	4.61	nd
48	**3n**	Cl	OCH_2OMe	23%	7.00	nd
49	**3o**	Cl	OCH_2SMe	8.6%	6.50	nd
50	**7**	Cl	OCH_2CN	17%	7.34	nd
51	**9**	Cl	OPh	0%	5.39	nd
Class V						
52	**11a**	Cl	NHMe	5.39	8.06	2.67
53	**11b**	Cl	NHEt	5.03	7.55	2.53
54	**11c**	Cl	NH^iPr	0%	5.11	nd
55	**11d**	Cl	NHPh	0%	5.01	nd
56	**10b**	Cl	$NHCOCH_3$	6.55	7.41	0.86
57	**10c**	Cl	NHCOOEt	21%	6.23	nd
58	**10d**	Cl	NHCONHEt	0%	4.50[e]	nd
Class VI						
59	**3p**	Cl	OCH_2COCH_3	22%	7.57	nd
60	**5a**	Cl	OCH_2COOH	0%	4.50[e]	nd
61	**4a**	Cl	OCH_2COOEt	0%	5.74	nd
62	**6b**	Cl	OCH_2CONH_2	4.62	8.48	3.86
63	**6a**	Br	OCH_2CONH_2	5.05	8.05	3.00
64	**6c**	Cl	$OCH_2CONHMe$	11%	7.47	nd
65	**6d**	Cl	$OCH_2CON(Me)_2$	10%	6.30	nd
66	**6e**	Cl	OCH_2CO-1′-piperidinyl	9.0%	4.41	nd
67	**6f**	Cl	OCH_2CO-4′-morpholinyl	3.2%	4.89	nd

[a] Entry numbers used in the section "Results and discussion".
[b] Compound numbers used for the section "Chemistry" and "Experimental section".
[c] MAO-A and MAO-B inhibitory activities are expressed as pIC_{50} or as percentage of inhibition at 10 μM. Values are the mean of two or three independent experiments.
[d] SI, is the selectivity index expressed as pIC_{50} MAO-B−pIC_{50} MAO-A (ΔpIC_{50}); nd = not determined.
[e] Estimated value from the % of inhibition at 10 μM concentration (see text).

3. Biological assays

The inhibition of monoamine oxidases A and B activity was measured in vitro by using crude rat brain mitochondrial homogenates through a spectrophotometric method [44] based on the monitoring of the oxidation rate of the non-selective non-fluorescent MAO substrate kynuramine to 4-hydroxyquinoline. The percentage of MAO inhibition was determined for all the examined compounds at 10 μM concentration and IC_{50} data were measured only for compounds showing an inhibition greater than 50%. In a few cases the IC_{50} was measured also for compounds with low activity (MAO-I < 50% at 10 μM) when deemed necessary for a quantitative evaluation of the structure-activity and/or structure–selectivity relationships (SAR and SSR respectively). Inhibitory potency was expressed as pIC_{50} and the selectivity index (SI) as the difference pIC_{50} MAO-B−pIC_{50} MAO-A (ΔpIC_{50}). pIC_{50}s, SIs and % of MAO inhibition are reported in Table 1 along with the chemical structures of the examined 4,7-disubstituted coumarins. To avoid the loss of important structural information in the derivation of sound SAR, for the low active acid (entries 15 and 60 in Table 1) and ureido (entry 58) MAO-B inhibitors, estimated pIC_{50} values of 4.0 and 4.5 were used, respectively.

4. Molecular modelling studies

The need to clarify at a 3D level some important molecular aspects of previously discussed SAR, prompted us to undertake a number of docking simulations to better assess, at the MAO-B binding site, the effect on binding of some examined substituents at position 4 of coumarin. The steric effect was analyzed in terms of both posing and scoring by investigating the nature of the binding interactions along with an analysis of the enzymatic room available at position 4 and the subtle conformational rearrangements experienced by the 4-substituents. Besides the steric effect, docking models permitted to clearly spot enzymatic regions where the occurrence of HBD interactions can enhance the MAO-B affinity.

5. Results and discussion

A preliminary search to identify the best anchoring substituent at position 7 for high potency and selectivity towards MAO-B, was carried out on the basis of previous SARs and X-ray data from a molecular complex of entry 13 with human MAO-B. Since previous SARs suggested a halogen atom at meta-position as the best substituents in the 7-benzyloxy group, F, Cl and Br were selected as suitable binding elements. To keep the overall molecular lipophilicity at an acceptable level, the inhibitory potency of 7-

benzyloxy derivatives bearing in the meta positions F, Cl and Br substituents was firstly measured on coumarins carrying at position 4 substituents with increasing lipophilicity, that is OH (entries 8–11), OMe (entries 35–38), OEt (entries 39–42), and O^{n}Pr (entries 43–46). Comparative analysis of the resulting inhibition data (see infra) suggested the 3-chloro atom on the benzyloxy moiety as the ideal substituent ensuring both comparable potency and lower lipophilicity than the corresponding 3-bromo substituted analogues.

The 3-chorobenzyloxy substituent was therefore kept constant in the design of all the other 4-substituted coumarins reported in Table 1. Since in previous studies the substituent effects on MAO affinity and selectivity at 4-, and to lesser extent, 3-position, have been mainly assessed with hydrophobic substituents, in the present work polar substituents with different conformational, hydrophobic, electronic and steric properties were investigated. Bulky substituents carrying aliphatic or cycloaliphatic moieties were introduced at position 4 to better assess the steric effects.

Possible metabolic transformations of one substituent/molecule to another through demethylation, deacylation, hydrolysis and oxidation reactions were also considered in the molecular design to prospect the in vivo behaviour of lead inhibitors.

5.1. SAR and SSR

For a better analysis and discussion of the SARs and SSRs, 7-(meta-halogenobenzyloxy)-4-substituted coumarins in Table 1 were divided in six different classes as follows: Class I, comprising lead compound (entry 1) and compounds bearing small hydrophobic substituents at position 4 (entries 2–7); Class II, containing small polar groups directly linked at the C-4 (entries 8–19); Class III, containing 4-CH_2R groups (entries 20–34) where R is a polar substituent; Class IV, containing 4-alkoxy groups and a 4-phenoxy group (entries 35–50 and 51, respectively); Class V, comprising 4-NHR and 4-NHCOR groups (entries 52–55 and 56–58, respectively) and Class VI, collecting compounds with 4-OCH_2COR groups (entries 59–67) where R is a polar substituent. For a rapid visual inspection of MAO-B affinity distribution over the different classes, pIC_{50} values were plotted as a histogram in Fig. 1. The limited availability of MAO-A pIC_{50} makes useless a similar representation for MAO-A inhibition.

At a first glance, inhibition data in Fig. 1 and Table 1 indicate that very potent and selective MAO-B inhibitors were discovered and that no apparent relationship exists between MAO-A and MAO-B inhibitory potency. MAO-A affinity was generally very low and only in a very few cases a sub-micromolar IC_{50} value was observed (i.e., entries 23, 25 and 56). The most potent MAO-B inhibitors ($pIC_{50} \geq 7.80$) were entries 2, 20, 21, 23, 27–29, 37, 38, 52, 62 and 63 which were distributed nearly over all the classes of compound in Table 1 but prevalently within class III (see Fig. 1). Entry 62, that is the 4-oxyacetamido-7-metachlorobenzyloxy coumarin, resulted the most potent and selective MAO-B inhibitor of the whole series of examined compounds, exhibiting outstanding pIC_{50} and SI values equal to 8.48 and 3.86, respectively.

Anionic carboxylic acid derivatives (entries 15 and 60) displayed almost no MAO inhibition. Interestingly, some inhibitory activity towards MAO-B was recovered in the corresponding ethyl esters (entries 16 and 61, respectively).

4-OH coumarin derivatives, which at physiological pH are fully ionized, exhibited low MAO-B inhibition for the 3′-unsubstituted- and 3′-fluoro-benzyloxy derivatives (entries 8 and 9, respectively) whereas a higher and nearly identical, sub-micromolar inhibitory activity at MAO-B was displayed by the 3′-chloro- and 3′-bromo-benzyloxy congeners (entries 10 and 11, respectively). As foreseeable, the substitution of the highly polar anionic 4-OH group with linear alkoxy groups afforded a series of potent and selective MAO-B inhibitors. These MAO-B inhibition data prompted us to choose the 3′-chlorobenzyloxy substituent at position 7 of the coumarin ring as the most efficient anchoring moiety to the MAO-B binding site while introducing a large variety of substituents at position 4 to thoroughly exploit the physicochemical and spatial binding domain of that region.

The following discussion of the SAR within the classes of inhibitors I–VI was limited to MAO-B inhibition because MAO-A pIC_{50} were available only for a limited number of compounds.

5.2. Inhibitors of class I

MAO-B Inhibitory potency of compounds of class I appeared to be mainly modulated by steric effects. Taft Es steric parameters are linearly related to the inhibitory potency (data not shown), being the unsubstituted entry 1 an underpredicted outlier.

The most potent inhibitors are the 4-Me and 4-Cl coumarin derivatives (entries 2 and 5, respectively). As it will be seen later also for other classes of compounds reported herein, substituent steric effects seemed to be the most relevant modulators of MAO-B inhibitory potency.

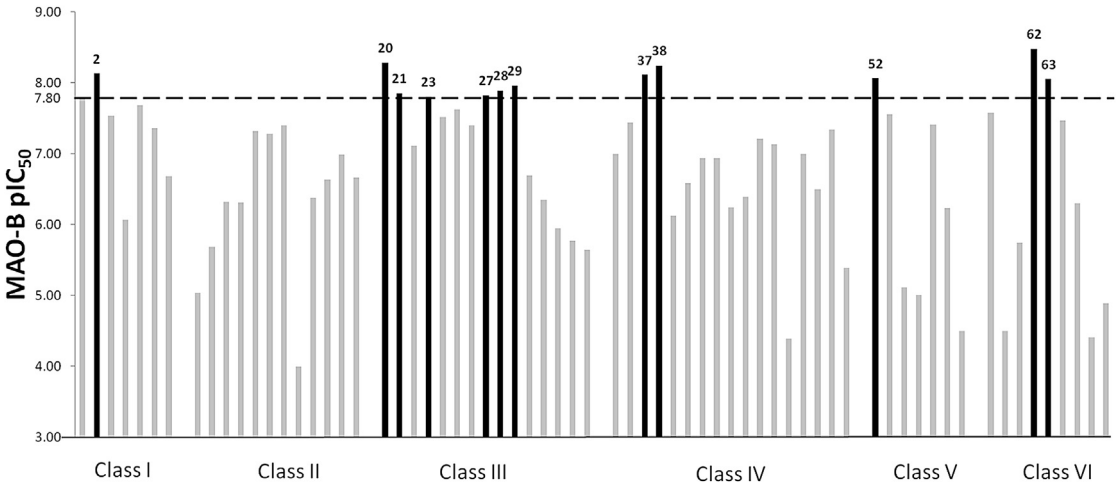

Fig. 1. pIC_{50}s values distribution within the different classes of coumarin MAO-B inhibitors. Highly potent inhibitors ($pIC_{50} \geq 7.80$) are highlighted with black bars.

5.3. Inhibitors of class II

The fully ionized 4-enol (entries 8–11) and 4-carboxy (entry 15) coumarin derivatives exhibited a very low inhibitory potency. As anticipated in the general discussion, the affinity of the 4-OH derivatives increased with the increase of the lipophilic character of the meta substituent of the benzyloxy group. Small hydrophilic substituents at position 4 displayed a good inhibitory potency (see entries 12–14 and 18) whereas compound **16**, bearing the larger and more lipophilic carbethoxy substituent, was the less active inhibitor among the unionized compounds of this series.

5.4. Inhibitors of class III

R groups of the 4-CH_2R moiety are very polar and mainly represented by diversely substituted amino groups (see entries 27–34). Very small and polar R groups (i.e., OH, CN, NH_2, $NHCH_3$, $CONH_2$, and $CONHCH_3$) characterize compounds with a very high MAO-B inhibitory potency. However a comparable activity was also observed for the corresponding 4-CH_2Cl (entry 6) and this suggested that in the "R region" small, highly polar or lipophilic groups can be easily accommodated. As described in the modelling section, different interactions could take place and contribute to the binding affinity.

It is worth noting that position 4 did not tolerate bulky groups as can be inferred comparing the affinities of entry 27 bearing an *N*-methyl amino group with the corresponding *N*-monoalkyl substituted congeners (entries 28, 30 and 31) and the *N*,*N*-disubstituted congeners (entries 32–34) bearing alkyl and cyclolakyl groups of increasing size. Actually entries 33 and 34 bearing the bulky pyrrolidine and morpholine rings are the least potent MAO-B inhibitors within this class of derivatives with pIC_{50} values equal to 5.77 and 5.64, respectively.

5.5. Inhibitors of class IV

Among 4-alkoxy coumarins (entries 35–49), methoxy derivatives (entries 35–38) exhibited the highest activity being the 3′-chloro- and 3′-bromobenzyloxy congeners two of the most potent and selective MAO-B inhibitors of the whole series of studied compounds (i.e., pIC_{50} = 8.24 and 8.11; SI = 3.18 and SI > 3.24, respectively). In general, in the three different series of 4-alkoxy coumarins, that is 4-methoxy, 4-ethoxy and 4-*n*-propoxy, the following rank of activity was observed 3′-ClOBn ≥ 3′-BrOBn > 3′-FOBn > 3′-unsubstituted OBn. These findings were slightly surprising because a significant increase of activity was expected from the interaction of the more lipophilic 3-BrOBn derivatives, compared to the corresponding 3′-ClOBn derivatives, in the lipophilic pocket of the MAO-B binding site, well delineated by X-ray crystallography of the complexes of entry 13, safinamide and coumarin NW-1772 with MAO-B [43]. MAO-B inhibitory potency of 4-alkoxy coumarins bearing a 7-(3′-chlorobenzyloxy) group was ranked as follows: 4-OMe > 4-O^{n}Pr > 4-OEt >> 4-O^{i}Pr and this was again indicative of a strong steric effect at position 4. Actually, the inhibitory potency of the 4-isopropoxy derivative, entry 47, was 3141-fold lower than that of the 4-methoxy analogue (entry 37). The isosteric substitution of one methylene group of the *n*-propoxy (entry 45) with one oxygen (entry 48) or one sulphur atom (entry 49) led to a decrease of activity, especially for compound **49** which showed a 5-fold decrease of potency (pIC_{50} = 6.50 vs 7.21). To explain these data as well as the very low activity observed for the 4-phenoxy derivative (entry 51, pIC_{50} = 5.39) again a steric effect could be advocated. Interestingly a good linear relationship (data not shown) can be found between inhibitory potency and the ν steric parameter of Charton [45] for the 4-alkoxy coumarins bearing a 7-(3′-chlorobenzyloxy) group **37**, **41**, **45** and **47**–**50**. The 4-OCH_2CN derivative (entry 50, pIC_{50} = 7.34) was a strong outlier and was discarded from the regression analysis as it showed a very high activity despite a steric hindrance higher than its OEt analogue (entry 41). It may be speculated that the CN group might be involved in the formation of a HB reinforcing the inhibitor binding to MAO-B.

5.6. Inhibitors of class V

Despite the limited number of 4-NHR and 4-NHCOR derivatives prepared and tested, also for this class of inhibitors a clear steric effect of the R substituent was detected being the compounds with bulkier substituents (i.e., entries 54, 55, 57 and 58) the least active of the series. It is worth noting that the 4-NHAc derivative (entry 56) displayed the highest MAO-A inhibitory potency (pIC_{50} = 6.55 and, consequently, a very low selectivity index, SI = 0.86).

5.7. Inhibitors of class VI

Also for this class of compounds, that is 4-OCH_2COR substituted derivatives, steric hindrance of the R group plays a key role in the modulation of MAO-B inhibitory potency. Actually, entries 59 and 62–64, bearing small R groups, exhibited the highest MAO-B inhibitory activity whereas compounds carrying bulkier groups (e.g., the ethyl ester **61** and the *N*,*N*-dimethyl-, piperidine- and morpholine-amides **65**–**67**) showed a very low inhibitory potency. Also for these compounds the decrease of activity seemed to be directly correlated to the steric hindrance of the R group being more pronounced for the bulkiest piperidine and morpholine groups present in entries 66 and 67 (pIC_{50} = 4.41 and 4.89, respectively). As already mentioned, the anionic 4-oxyacetic acid derivative **60** showed no affinity for both MAO isoforms. Remarkably, the most potent and selective MAO-B inhibitor, that is the 7-(3′-chlorobenzyloxy)-4-oxyacetamido coumarin **62** (pIC_{50} = 8.48, SI = 3.86) was found in this class of inhibitors. Its corresponding 3′-bromobenzyloxy analogue **63** displayed a slightly lower inhibitory potency (pIC_{50} = 8.05) and a significantly lower selectivity index (SI = 3.00) thus confirming the correctness of our selection of the 3′-chlorobenzyloxy substituent a the position 7 of the coumarin ring as the ideal binding moiety for a high MAO-B inhibitory potency and MAO-B over MAO-A selectivity.

Previous analysis and discussion of SARs pointed out the importance of steric effects at position 4 and lipophilic effects at the meta position of the 7-benzyloxy group, providing significant insights on the pivotal physicochemical interactions taking place at the MAO-B binding site. However, the lack of suitable electronic, lipophilic and hydrogen bonding parameters for most of the explored 4-substituents precluded the derivation of a more general, comprehensive and informative QSAR model. Consequently, to detect and locate at the three-dimensional level possible additional interactions driving the ligand binding at position 4, inhibition data of some selected inhibitors were modelled through docking simulations.

6. Docking simulations

Docking simulations aimed to explain mainly the drop of affinity caused by the introduction of bulky substituents at position 4 of the coumarin ring (e.g., entry 20 vs 66) strictly related to the limited steric accessibility of the MAO-B binding counterpart. A number of derivatives, of which some have at position 4 branched or cyclic bulky groups (i.e., entries 6, 20, 33, 34, 51, 54, 62 and 66), were selected and their binding interactions evaluated through docking studies. The GOLD 5.1 [46] program was used to carry out docking

simulations, since in several studies it yielded better performances compared to other similar programs. Given that our MAO-B inhibition data were determined on rat brain mitochondria homogenates, docking simulations were run on homology model of rat MAO-B isoform, for which no crystallographic data were available. As reported in our previous papers [33,39], eight structural water molecules were explicitly taken into account in the docking screens, and a conformational flexibility was allowed to two critical residues, Q206 and Y398, through the exploration of a rotamer library of GOLD software.

Results from our docking screen pointed out the steric hindrance of the 4-substituents as a clear molecular determinant influencing the MAO-B inhibitory potency. In this respect, the structural water molecules might play a role also in forcing highly branched or bulky substituents to folded conformations at the expense not only of their energetic content but also of their chance of establishing favourable hydrogen bonds with ordered water molecules. Satisfactorily, a good agreement was observed between experimental inhibitory activities and docking scoring values. As shown in Fig. 2a, one of the most active compound (entry 20, $pIC_{50} = 8.28$), bearing the small hydroxymethyl group at position 4, was well accommodated in the MAO-B binding site and was involved in a stabilizing HB network including at least three structural water molecules as shown in Fig. 2. A docking score as high as 79.85 kJ/mol was calculated. Replacing the hydroxyl with the chlorine atom led to a slight decrease of activity (entry 6, $pIC_{50} = 7.36$) likely due to the loss of HB interactions yielding to a lower docking score (76.61 kJ/mol). On the other hand, the flexibility of the larger polar group at position 4 of the most active inhibitor (entry 62, $pIC_{50} = 8.48$) ensured the occurrence of an HB with a specific amino acid residues resulting in a high docking score value (74.76 kJ/mol). As anticipated, the introduction of bulkier groups had the effect of strongly lowering the docking score. For instance, the consistent loss of activity of piperidine derivative (entry 66, $pIC_{50} = 4.41$) was likely due to the need of rearranging in a high-energy folded conformation yielding a score as low as 34.79 kJ/mol despite, as shown in Fig. 2b, the displacement of Y398 from its native position to reduce possible steric clashes. Although less pronounced, a similar behaviour was experienced by other cyclic part of 4-substituents in the search of larger room into the MAO-B binding site. The relevant drop of activity due to the introduction of the morpholinyl (entry 34, $pIC_{50} = 5.64$) and pyrrolidinyl (entry 33, $pIC_{50} = 5.77$) rings had a clear negative impact on the docking score lowered to 56.14 kJ/mol and 66.87 kJ/mol, respectively. The docking poses (data not shown) confirmed the hypothesized conformational rearrangements visited by those cyclic substituents.

7. Conclusions

Small sized hydrophobic and polar substituents, including the aliphatic charged amino groups, were well tolerated at the position 4 of 7-benzyloxy coumarins. Compounds bearing highly polar and anionic 4-substituents were instead disallowed. The systematic and finely-tuned exploration of position 4 allowed a very precise detection of the physicochemical features of the admitted substituents. In particular docking simulations helped to detect and locate at the 3D level the main steric, hydrophobic, and HB interactions underlying the selective MAO-B inhibition potency. The prevalent role of steric interactions was clearly pointed out along with the important role of hydrophobic interactions, chiefly of the 7-meta-substituted benzyloxy groups, previously observed for coumarins [47] and condensed diazine derivatives [48].

Interestingly, many substituents were designed as metabolically-related moieties (e.g., 4-CH_3, 4-CH_2OH, 4-CHO and 4-COOH; 4-$N(CH_3)_2$, 4-$NHCH_3$, 4-NH_2 and 4NHAc; 4-$XCH_2CON(CH_3)_2$ and 4-$XCH_2CONHCH_3$; 4-OCH_3 and 4-OH) and this may help the reliable prediction of the activity of putative metabolites of the most interesting parent inhibitors.

The large variety of substituents at position 4 characterizing highly potent and selective MAO-B inhibitors may enable the selection of the most appropriate compounds for safe and site-selective delivery (e.g., at CNS), for a long- or short-lasting action (high or low metabolic stability) and/or for the eventual preparation of suitable pro-drugs (e.g., from amine **13e** and alcohol **13d**).

The main outcomes from our SAR and docking studies might help the design of new and selective MAO-B inhibitors based on heterocyclic scaffold different from coumarins (scaffold hopping) [33] and eventually multimodal drugs addressing other biochemical targets relevant for NDs diseases along MAO-B. Indeed, long-term studies are going on in our laboratories to address NDs through a multitarget-directed-ligand approach [49]. Some encouraging preliminary results have been reported [50] and

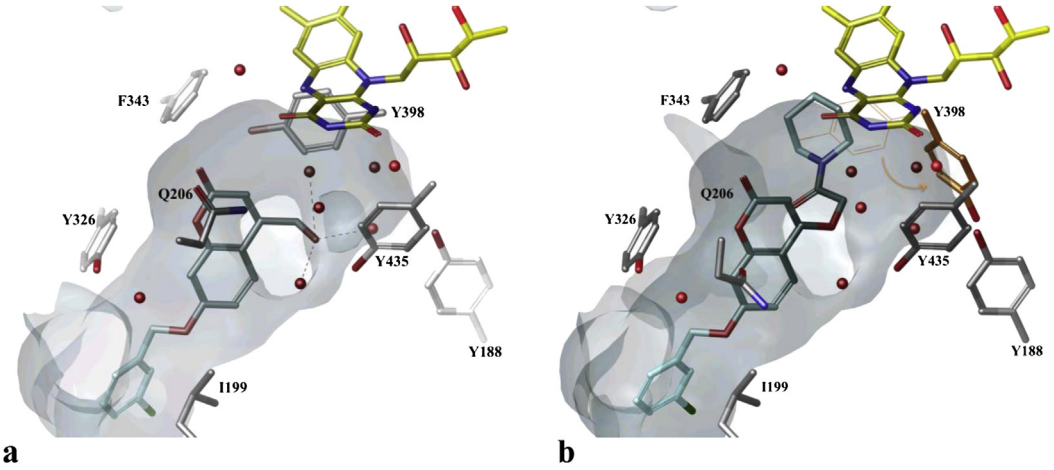

Fig. 2. Top-ranked docking pose of entries 20 (a) ($pIC_{50} = 8.28$) and 66 (b) ($pIC_{50} = 4.41$) into rMAO-B binding site. Relevant amino acid side chains, FAD cofactor, and inhibitors are represented as stick models coloured according to the following atom code: C atoms in white, yellow, and cyan for amino acid side chains, cofactor and inhibitor, respectively. Ordered water molecules are represented as red balls. The protein binding site is rendered as a light blue surface. (a) The black dashed lines indicate the HB network established by entry 20 with ordered water molecules. (b) The orange wireframe and stick model of Y398 indicate its native and rotated conformations following docking optimization of the piperidinyl inhibitor **6e** (entry 66). (For interpretation of the references to colour in this figure legend, the reader is referred to the web version of this article.)

original insights from the present work will help the design of new, in vivo-active, multitarget-directed ligands having the selective MAO-B inhibition as the core biological activity [30].

8. Experimental section

8.1. Chemistry

Starting materials, reagents and analytical grade solvents were purchased from Sigma–Aldrich (Europe). The purity of all the intermediates, checked by ^{1}H NMR and HPLC was always better than 95%. Column chromatography was performed using Carlo Erba silica gel (0.05–0.20 mm) or Carlo Erba neutral aluminium oxide (Brockmann activity I). Flash chromatographic separations were performed on Biotage SP1 purification system using flash cartridges prepacked with KP-Sil 32–63 μm, 60 Å silica. All reactions were routinely checked by TLC using Merck Kieselgel 60 F_{254} aluminium plates and visualized by UV light or iodine. Regarding the reaction requiring the use of dry solvents, the glassware was flame-dried and then cooled under a stream of dry argon before the use. Microwave reactions were performed in a Milestone MicroSynth apparatus, setting temperature and hold times, fixing maximum irradiation power to 500 W and heating ramp times to 2 min. Elemental analyses were performed on the Carlo Erba Elemental Analyzer Model EA 1110 or EuroEA 3000 analyzer only on the final compounds tested as MAOs inhibitors. The measured values for C, H, and N agreed to within ±0.40% of the theoretical values. Nuclear magnetic resonance spectra were recorded on a Varian Mercury 300 instrument (at 300 MHz) or on a Varian Gemini 200 instrument (at 200 MHz) at ambient temperature in the specified deuterated solvent. Chemical shifts (δ) are quoted in parts per million (ppm) and are referenced to the residual solvent peak (when registered at 300 MHz) or using $(CH_3)_4Si$ as an internal reference ($\delta = 0$, when recorded at 200 MHz). The coupling constants J are given in Hertz (Hz). The following abbreviations were used: s (singlet), d (doublet), dd (doublet of doublet), t (triplet), q (quadruplet), quint (quintet), sext (sextet), m (multiplet), br (broad signal); signals due to OH and NH protons were located by deuterium exchange with D_2O. Melting points were determined by the capillary method on a Stuart Scientific SMP3 electrothermal apparatus or using a Fisher-Johns apparatus and are uncorrected. Synthesis, analytic and spectroscopic data of compounds **1a** [41], **2a** [41], **12b** [42], **12c** [39], **12d** [43], **13a** [39], **13e–g** [39], **19** [33] and **25–28** (corresponding to entries 23–26 in Table 1) have been already reported in the literature. Coumarin **12a** was from commercial source.

8.1.1. General procedure for the synthesis of substituted acetophenones ***1b–d***

A mixture of 1-(2,4-dihydroxyphenyl)ethanone (3.0 g, 20 mmol), 20 mmol of the proper benzyl halide, 14.5 mmol (2.0 g) of anhydrous K_2CO_3 and 2-butanone (100 mL) was heated at reflux for 24 h with stirring. The mixture was then poured into cold water (500 mL) and exhaustively extracted with a mixture ethyl acetate–diethyl ether (1:1, v/v). The residue obtained from the combined extracts (washed with water and dried over anhydrous Na_2SO_4) was concentrated under reduced pressure and then purified through column chromatography on a silica gel column eluting with dichloromethane–petroleum ether (1:1, v/v), to recover pure compounds **1b–d** as white solids which were then crystallized from a suitable solvent.

*8.1.1.1. 1-{4-[(3-Fluorobenzyl)oxy]-2-hydroxyphenyl}ethanone (**1b**).* White solid; yield: 47%; mp: 108–9 °C (diisopropyl ether/petroleum ether). ^{1}H NMR (200 MHz, $CDCl_3$) δ: 2.56 (s, 3H), 5.09 (s, 2H), 6.47 (d, $J = 2.4$ Hz, 1H), 6.52 (dd, $J_1 = 2.4$ Hz, $J_2 = 8.8$ Hz, 1H), 6.99–7.07 (m, 1H), 7.11–7.21 (m, 1H), 7.32–7.40 (m, 2H), 7.65 (d, $J = 8.8$ Hz, 1H), 12.73 (s, 1H, dis. with D_2O).

*8.1.1.2. 1-{4-[(3-Chlorobenzyl)oxy]-2-hydroxyphenyl}ethanone (**1c**).* White solid; yield: 56%; mp: 127–8 °C (diisopropyl ether). ^{1}H NMR (200 MHz, $CDCl_3$) δ: 2.59 (s, 3H), 5.05 (s, 2H), 6.50 (d, $J = 2.4$ Hz, 1H), 6.54 (dd, $J_1 = 2.4$ Hz, $J_2 = 8.8$ Hz, 1H), 7.22–7.40 (m, 3H), 7.48 (s, 1H), 7.68 (d, $J = 8.8$ Hz, 1H), 12.77 (s, 1H, dis. with D_2O).

*8.1.1.3. 1-{4-[(3-Bromobenzyl)oxy]-2-hydroxyphenyl}ethanone (**1d**).* White solid; yield: 94%; mp: 141–2 °C (diisopropyl ether). ^{1}H NMR (200 MHz, $CDCl_3$) δ: 2.57 (s, 3H), 5.06 (s, 2H), 6.47 (d, $J = 2.4$ Hz, 1H), 6.51 (dd, $J_1 = 2.4$ Hz, $J_2 = 8.8$ Hz, 1H), 7.23–7.36 (m, 2H), 7.48 (m, 1H), 7.58 (s, 1H), 7.65 (d, $J = 8.8$ Hz, 1H), 12.73 (s, 1H, dis. with D_2O).

8.1.2. General procedure for the synthesis of 7-substituted-4-hydroxy-2H-chromen-2-ones ***2b–d***

A mixture of the proper 4-benzyloxy-2-hydroxyacetophenone **1b–d** (10 mmol), sodium (0.58 g, 25 mmol), diethyl carbonate (3.5 g, 30 mmol) and Dowtherm A (10 mL) was heated at 160 °C with stirring. Within a few minutes, after the sodium melting, a sudden reaction occurred with gas evolution and formation of an abundant whitish precipitate. Xylene (30 mL) was added in order to dilute the mixture and allow a better stirring, then the mixture was further heated at 160 °C for 1 h. After cooling, diethyl ether (30 mL) was added and the solid (nearly pure compound **2b–d** as sodium salts) was collected by filtration, washed with abundant diethyl ether and dried. Because in the subsequent synthetic step (*O*-alkylation) compounds **2b–d** were used as sodium salts, a major amount of the crude reaction product was stored just as was obtained, whereas a minor amount was dissolved in water (50 mL) and the alkaline aqueous solution was acidified with 6 N aqueous HCl so that compounds **2b–d** separated out as amorphous solids which were collected by filtration, washed with a little water, dried and crystallized from the proper solvent.

*8.1.2.1. 7-[(3-Fluorobenzyl)oxy]-4-hydroxy-2H-chromen-2-one (**2b**).* White crystals; yield: 66%; mp: 294–5 °C dec. (ethanol). ^{1}H NMR (300 MHz, DMSO-d_6) δ: 5.22 (s, 2H), 5.43 (s, 1H), 6.98 (d, $J = 2.5$ Hz, 1H), 7.02 (dd, $J_1 = 2.5$ Hz, $J_2 = 8.5$ Hz, 1H), 7.16–7.20 (m, 1H), 7.28–7.31 (m, 2H), 7.40–7.48 (m, 1H), 7.71 (d, $J = 8.5$ Hz, 1H), 12.36 (s, 1H, dis. with D_2O). Anal. ($C_{16}H_{11}FO_4$) C, H.

*8.1.2.2. **7**-[(3-Chlorobenzyl)oxy]-4-hydroxy-2H-chromen-2-one (**2c**).* White crystals; yield: 85%; mp: 261–3 °C dec. (acetone). ^{1}H NMR (300 MHz, DMSO-d_6) δ: 5.22 (s, 2H), 5.42 (s, 1H), 6.98 (d, $J = 2.2$ Hz, 1H), 7.02 (dd, $J_1 = 2.2$ Hz, $J_2 = 8.4$ Hz, 1H), 7.39–7.44 (m, 3H), 7.53 (s, 1H), 7.71 (d, $J = 8.4$ Hz, 1H), 12.35 (s, 1H, dis. with D_2O). Anal. ($C_{16}H_{11}ClO_4$) C, H.

*8.1.2.3. 7-[(3-Bromobenzyl)oxy]-4-hydroxy-2H-chromen-2-one (**2d**).* White crystals; yield: 83%; mp: 291–2 °C dec. (ethanol/acetone). ^{1}H NMR (200 MHz, DMSO-d_6) δ: 5.24 (s, 2H), 5.47 (s, 1H), 6.95–7.06 (m, 2H), 7.32–7.62 (m, 3H), 7.70 (s, 1H), 7.74 (d, $J = 8.8$ Hz, 1H), 12.15–12.80 (br s, 1H, dis. with D_2O). Anal. ($C_{16}H_{11}BrO_4$) C, H.

8.1.3. General procedure for the synthesis of 7-(benzyloxy)-4-alkoxy-2H-chromen-2-ones ***3a–c*** and 7-[(3-halobenzyl)oxy]-4-alkoxy-2H-chromen-2-ones ***3d–p***

A large excess (1.0 mL) of the proper alkyl halide was added to the solution of the sodium salt of compounds **2a–d** (1.0 mmol) in 25 mL of dry DMF and the mixture was stirred at room temperature for 1.5 h, then poured into cold water. The resulting emulsion was

exhaustively extracted with the mixture diethyl ether–ethyl acetate (1:1, v/v). The combined extracts (dried over anhydrous Na_2SO_4 and evaporated to dryness at reduced pressure) afforded a thick oil which was chromatographed on a silica gel column eluting with CH_2Cl_2. The fraction collected, after removal of solvents, gave pure compounds **3a**–**p** as white solids which were then crystallized from proper solvents.

*8.1.3.1. 7-(Benzyloxy)-4-methoxy-2H-chromen-2-one (**3a**).* White crystals; yield: 60%; mp: 141–3 °C (ethyl acetate/petroleum ether). ^{1}H NMR (200 MHz, $CDCl_3$) δ: 3.96 (s, 3H), 5.11 (s, 2H), 5.56 (s, 1H), 6.85 (d, J = 2.4 Hz, 1H), 6.90 (dd, J_1 = 2.4 Hz, J_2 = 8.8 Hz, 1H), 7.31–7.46 (m, 5H), 7.69 (d, J = 8.8 Hz, 1H). Anal. ($C_{17}H_{14}O_4$) C, H.

*8.1.3.2. 7-(Benzyloxy)-4-ethoxy-2H-chromen-2-one (**3b**).* White crystals; yield: 57%; mp: 132–3 °C (diisopropyl ether). ^{1}H NMR (300 MHz, $CDCl_3$) δ: 1.52 (t, J = 6.9 Hz, 3H), 4.18 (q, J = 6.9 Hz, 2H), 5.12 (s, 2H), 5.54 (s, 1H), 6.86 (d, J = 2.2 Hz, 1H), 6.91 (dd, J_1 = 2.2 Hz, J_2 = 8.8 Hz, 1H), 7.33–7.45 (m, 5H), 7.73 (d, J = 8.8 Hz, 1H). Anal. ($C_{18}H_{16}O_4$) C, H.

*8.1.3.3. 7-(Benzyloxy)-4-propoxy-2H-chromen-2-one (**3c**).* White crystals; yield: 48%; mp: 107–8 °C (diisopropyl ether). ^{1}H NMR (300 MHz, $CDCl_3$) δ: 1.09 (t, J = 7.4 Hz, 3H), 1.91 (sext, J = 7.4 Hz, 2H), 4.06 (t, J = 7.4 Hz, 2H), 5.12 (s, 2H), 5.54 (s, 1H), 6.86 (d, J = 2.5 Hz, 1H), 6.91 (dd, J_1 = 2.5 Hz, J_2 = 8.8 Hz, 1H), 7.33–7.45 (m, 5H), 7.72 (d, J = 8.8 Hz, 1H). Anal. ($C_{19}H_{18}O_4$) C, H.

*8.1.3.4. 7-[(3-Fluorobenzyl)oxy]-4-methoxy-2H-chromen-2-one (**3d**).* White crystals; yield: 76%; mp: 142–3 °C (diisopropyl ether). ^{1}H NMR (200 MHz, $CDCl_3$) δ: 4.00 (s, 3H), 5.15 (s, 2H), 5.60 (s, 1H), 6.82–7.48 (m, 6H), 7.74 (d, J = 8.8 Hz, 1H). Anal. ($C_{17}H_{13}FO_4$) C, H.

*8.1.3.5. 4-Ethoxy-7-[(3-fluorobenzyl)oxy]-2H-chromen-2-one (**3e**).* White crystals; yield: 73%; mp: 123–5 °C (diisopropyl ether/petroleum ether). ^{1}H NMR (200 MHz, $CDCl_3$) δ: 1.55 (t, J = 7.0 Hz, 3H), 4.21 (q, J = 7.0 Hz, 2H), 5.15 (s, 2H), 5.58 (s, 1H), 6.82–7.53 (m, 6H), 7.78 (d, J = 8.8 Hz, 1H). Anal. ($C_{18}H_{15}FO_4$) C, H.

*8.1.3.6. 7-[(3-Fluorobenzyl)oxy]-4-propoxy-2H-chromen-2-one (**3f**).* White crystals; yield: 55%; mp: 99–100 °C (diethyl ether). ^{1}H NMR (300 MHz, $CDCl_3$) δ: 1.09 (t, J = 7.4 Hz, 3H), 1.92 (sext, J = 7.4 Hz, 2H), 4.07 (t, J = 7.4 Hz, 2H), 5.12 (s, 2H), 5.54 (s, 1H), 6.83 (d, J = 2.2 Hz, 1H), 6.90 (dd, J_1 = 2.2 Hz, J_2 = 8.8 Hz, 1H), 7.00–7.07 (m, 1H), 7.13–7.21 (m, 2H), 7.33–7.40 (m, 1H), 7.73 (d, J = 8.8 Hz, 1H). Anal. ($C_{19}H_{17}FO_4$) C, H.

*8.1.3.7. 7-[(3-Chlorobenzyl)oxy]-4-methoxy-2H-chromen-2-one (**3g**).* White crystals; yield: 92%; mp: 131–3 °C (ethyl acetate/petroleum ether). ^{1}H NMR (200 MHz, $CDCl_3$) δ: 4.00 (s, 3H), 5.12 (s, 2H), 5.60 (s, 1H), 6.82–6.98 (m, 2H), 7.30–7.40 (m, 3H), 7.46 (s, 1H), 7.74 (d, J = 8.8 Hz, 1H). Anal. ($C_{17}H_{13}ClO_4$) C, H.

*8.1.3.8. 7-[(3-Chlorobenzyl)oxy]-4-ethoxy-2H-chromen-2-one (**3h**).* White crystals; yield: 79%; mp: 128–130 °C (diisopropyl ether). ^{1}H NMR (200 MHz, $CDCl_3$) δ: 1.55 (t, J = 7.0 Hz, 3H), 4.21 (q, J = 7.0 Hz, 2H), 5.12 (s, 2H), 5.57 (s, 1H), 6.82–6.98 (m, 2H), 7.28–7.43 (m, 3H), 7.47 (s, 1H), 7.76 (d, J = 8.8 Hz, 1H). Anal. ($C_{18}H_{15}ClO_4$) C, H.

*8.1.3.9. 7-[(3-Chlorobenzyl)oxy]-4-propoxy-2H-chromen-2-one (**3i**).* White crystals; yield: 55%; mp: 108–9 °C (diisopropyl ether). ^{1}H NMR (200 MHz, $CDCl_3$) δ: 1.12 (t, J = 7.0 Hz, 3H), 1.95 (m, 2H), 4.10 (t, J = 7.0 Hz, 2H), 5.12 (s, 2H), 5.58 (s, 1H), 6.82–6.98 (m, 2H), 7.25–7.42 (m, 3H), 7.47 (s, 1H), 7.77 (d, J = 8.8 Hz, 1H). Anal. ($C_{19}H_{17}ClO_4$) C, H.

*8.1.3.10. 7-[(3-Bromobenzyl)oxy]-4-methoxy-2H-chromen-2-one (**3j**).* White crystals; yield: 64%; mp: 140–1 °C (CH_2Cl_2/petroleum ether). ^{1}H NMR (200 MHz, $CDCl_3$) δ: 4.00 (s, 3H), 5.12 (s, 2H), 5.61 (s, 1H), 6.82–6.98 (m, 2H), 7.23–7.42 (m, 2H), 7.52 (m, 1H), 7.63 (s, 1H), 7.74 (d, J = 8.8 Hz, 1H). Anal. ($C_{17}H_{13}BrO_4$) C, H.

*8.1.3.11. 7-[(3-Bromobenzyl)oxy]-4-ethoxy-2H-chromen-2-one (**3k**).* White crystals; yield: 64%; mp: 98.5–100 °C (diisopropyl ether). ^{1}H NMR (300 MHz, DMSO-d_6) δ: 1.38 (t, J = 7.2 Hz, 3H), 4.23 (q, J = 7.2 Hz, 2H), 5.21 (s, 2H), 5.72 (s, 1H), 6.99–7.07 (m, 2H), 7.33–7.39 (m, 1H), 7.45–7.48 (m, 1H), 7.53–7.55 (m, 1H), 7.67–7.69 (m, 1H), 7.70 (d, J = 1.9 Hz, 1H). Anal. ($C_{18}H_{15}BrO_4$) C, H.

*8.1.3.12. 7-[(3-Bromobenzyl)oxy]-4-propoxy-2H-chromen-2-one (**3l**).* White crystals; yield: 51%; mp: 113–4 °C (diisopropyl ether). ^{1}H NMR (300 MHz, $CDCl_3$) δ: 1.09 (t, J = 7.4 Hz, 3H), 1.93 (sext, J = 7.4 Hz, 2H), 4.07 (t, J = 7.4 Hz, 2H), 5.09 (s, 2H), 5.55 (s, 1H), 6.83 (d, J = 1.9 Hz, 1H), 6.90 (dd, J_1 = 1.9 Hz, J_2 = 8.8 Hz, 1H), 7.29–7.37 (m, 2H), 7.47–7.49 (m, 1H), 7.60 (s, 1H), 7.73 (d, J = 8.8 Hz, 1H). Anal. ($C_{19}H_{17}BrO_4$) C, H.

*8.1.3.13. 7-[(3-Chlorobenzyl)oxy]-4-isopropoxy-2H-chromen-2-one (**3m**).* White crystals; yield: 44%; mp: 137–8 °C (diisopropyl ether). ^{1}H NMR (200 MHz, $CDCl_3$) δ: 1.48 (d, J = 6.2 Hz, 6H), 4.73 (m, 1H), 5.12 (s, 2H), 5.57 (s, 1H), 6.82–6.98 (m, 2H), 7.28–7.42 (m, 3H), 7.47 (s, 1H), 7.75 (d, J = 8.8 Hz, 1H). Anal. ($C_{19}H_{17}ClO_4$) C, H.

*8.1.3.14. 7-[(3-Chlorobenzyl)oxy]-4-(methoxymethoxy)-2H-chromen-2-one (**3n**).* White crystals; yield: 69%; mp: 130–1 °C (ethyl acetate/petroleum ether). ^{1}H NMR (200 MHz, $CDCl_3$) δ: 3.57 (s, 3H), 5.13 (s, 2H), 5.37 (s, 2H), 5.81 (s, 1H), 6.82–6.98 (m, 2H), 7.26–7.42 (m, 3H), 7.47 (s, 1H), 7.77 (d, J = 8.8 Hz, 1H). Anal. ($C_{18}H_{15}ClO_5$) C, H.

*8.1.3.15. 7-[(3-Chlorobenzyl)oxy]-4-[(methylthio)methoxy]-2H-chromen-2-one (**3o**).* White crystals; yield: 33%; mp: 137–9 °C (ethyl acetate/petroleum ether). ^{1}H NMR (200 MHz, $CDCl_3$) δ: 2.36 (s, 3H), 5.13 (s, 2H), 5.28 (s, 2H), 5.62 (s, 1H), 6.82–6.98 (m, 2H), 7.22–7.40 (m, 3H), 7.47 (s, 1H), 7.77 (d, J = 8.8 Hz, 1H). Anal. ($C_{18}H_{15}ClO_4S$) C, H, S.

*8.1.3.16. 7-[(3-Chlorobenzyl)oxy]-4-(2-oxopropoxy)-2H-chromen-2-one (**3p**).* White crystals; yield: 31%; mp: 210–2 °C (ethyl acetate). ^{1}H NMR (200 MHz, $CDCl_3$) δ: 2.35 (s, 3H), 4.74 (s, 2H), 5.14 (s, 2H), 5.44 (s, 1H), 6.83–7.01 (m, 2H), 7.26–7.42 (m, 3H), 7.47 (s, 1H), 7.83 (d, J = 8.8 Hz, 1H). Anal. ($C_{19}H_{15}ClO_5$) C, H.

*8.1.4. General procedure for the synthesis of ethyl ({7-[(3-halobenzyl)oxy]-2-oxo-2H-chromen-4-yl}oxy)acetates **4a**,**b***

A mixture of the 4-hydroxycoumarin **2c** (1.0 g, 3.0 mmol) or **2d** (0.91 g, 3.0 mmol), ethyl bromoacetate (1.0 mL), anhydrous K_2CO_3 (1.0 g) and 2-butanone (25 mL) was heated at reflux for 3 h with stirring. The reaction mixture was poured into cold water (300 mL) and exhaustively extracted with ethyl acetate–diethyl ether (1:1, v/v). The combined extracts were washed with aqueous 1.0 N NaOH, then with water and dried over anhydrous Na_2SO_4. After removal of solvents, the oily residue was treated with a small amount of diethyl ether and petroleum ether so that the nearly pure compounds **4a**,**b** separated out as whitish solids.

*8.1.4.1. Ethyl ({7-[(3-chlorobenzyl)oxy]-2-oxo-2H-chromen-4-yl}oxy)acetate (**4a**).* White crystals; yield: 56%; mp: 135–6 °C (ethyl acetate). ^{1}H NMR (200 MHz, $CDCl_3$) δ: 1.36 (t, J = 7.0 Hz, 3H), 4.34 (q, J = 7.0 Hz, 2H), 4.77 (s, 2H), 5.13 (s, 2H), 5.48 (s, 1H), 6.84–7.00 (m, 2H), 7.27–7.42 (m, 3H), 7.47 (s, 1H), 7.85 (d, J = 8.8 Hz, 1H). Anal. ($C_{20}H_{17}ClO_6$) C, H.

*8.1.4.2. Ethyl ({7-[(3-bromobenzyl)oxy]-2-oxo-2H-chromen-4-yl} oxy)acetate (**4b**).* White crystals; yield: 73%; mp: 125–6 °C (ethyl acetate/petroleum ether). ^{1}H NMR (300 MHz, DMSO-d_6) δ: 1.22 (t, J = 7.2 Hz, 3H), 4.19 (q, J = 7.2 Hz, 2H), 5.04 (s, 2H), 5.22 (s, 2H), 5.76 (s, 1H), 7.05 (d, J = 2.5 Hz, 1H), 7.08 (dd, J_1 = 2.5 Hz, J_2 = 8.5 Hz, 1H), 7.36 (t, J = 7.7 Hz, 1H), 7.47 (d, J = 7.7 Hz, 1H), 7.53–7.56 (m, 1H), 7.68 (s, 1H), 7.73 (d, J = 8.5 Hz, 1H). Anal. ($C_{20}H_{17}BrO_6$) C, H.

*8.1.5. General procedure for the synthesis of ({7-[(3-halobenzyl) oxy]-2-oxo-2H-chromen-4-yl}oxy)acetic acids **5a**,**b***

Derivative **4a** (0.43 g, 1.0 mmol) or **4b** (0.39 g, 1.0 mmol) was added to an ethanolic solution of solid KOH (0.11 g, 2.0 mmol). Rapidly, the solution became yellow and a whitish solid (compounds **5a**,**b** as potassium salts) began to precipitate within few minutes. The suspension was kept stirring at room temperature for 1 h, then it was diluted with diethyl ether, filtered, washed with diethyl ether and dried. The potassium salts collected were dissolved in water and the resulting solution was acidified with 6 N HCl, so that the pure compound **5a** or **5b** separated out as a white solids which were collected by filtration, washed, with water, dried and crystallized from acetone.

*8.1.5.1. ({7-[(3-Chlorobenzyl)oxy]-2-oxo-2H-chromen-4-yl}oxy)acetic acid (**5a**).* White crystals; yield: 76%; mp: 228–230 °C (acetone). ^{1}H NMR (200 MHz, DMSO-d_6) δ: 4.90 (s, 2H), 5.26 (s, 2H), 5.69 (s, 1H), 7.01–7.16 (m, 2H), 7.37–7.53 (m, 3H), 7.58 (s, 1H), 7.78 (d, J = 8.8 Hz, 1H), OH not detected. Anal. ($C_{18}H_{13}ClO_6$) C, H.

*8.1.5.2. ({7-[(3-Bromobenzyl)oxy]-2-oxo-2H-chromen-4-yl}oxy)acetic acid (**5b**).* White crystals; yield: 72%; mp: 231–3 °C (acetone). ^{1}H NMR (300 MHz, DMSO-d_6) δ: 4.94 (s, 2H), 5.22 (s, 2H), 5.71 (s, 1H), 7.03–7.08 (m, 2H), 7.36 (t, J = 7.7 Hz, 1H), 7.47 (d, J = 7.7 Hz, 1H), 7.53–7.55 (m, 1H), 7.68 (s, 1H), 7.74 (d, J = 8.5 Hz, 1H), OH not detected. Anal. ($C_{18}H_{13}BrO_6$) C, H.

*8.1.6. General procedure for the synthesis of 2-({7-[(3-halobenzyl) oxy]-2-oxo-2H-chromen-4-yl}oxy)-N-alkylacetamides **6a**–**f***

$SOCl_2$ (20 mL) was added to the suspension of compound **5a** (0.40 g, 1.0 mmol) or **5b** (0.36 g, 1.0 mmol) in CH_2Cl_2 (25 mL) and the mixture was refluxed with stirring until a clear solution was obtained (~2 h). The solvent and the excess of $SOCl_2$ were then removed in vacuo and the resulting residue (crude acyl chloride of **5a** or **5b**) was cooled with an ice bath and treated with an excess of proper amine. In the case of **6a**,**b**, 15 mL of 30% aqueous ammonia were directly added to crude acyl chlorides and the resulting suspension was then stirred at room temperature for 30 min, then filtered to give the nearly pure compounds **6a** or **6b**. In all other cases, the ice-cooled acyl chloride of **5a** was treated with 5 mL of suitable amine dissolved in 30 mL of CH_2Cl_2. The resulting solution was stirred at room temperature for 30 min, then treated with aqueous 10% Na_2CO_3 (15 mL) and water (15 mL). The mixture was transferred in a separatory funnel, the organic solution was collected and the aqueous phase extracted twice with CH_2Cl_2. The combined extracts, after drying over anhydrous Na_2SO_4, were evaporated to dryness under reduced pressure to give an oily residue which was chromatographed on a silica gel column, eluting with the mixture CH_2Cl_2/ethyl acetate (1:1, v/v). The collected eluate afforded pure compounds **6c**–**f** as solids which were then crystallized from the proper solvent.

*8.1.6.1. 2-({7-[(3-Bromobenzyl)oxy]-2-oxo-2H-chromen-4-yl}oxy) acetamide (**6a**).* Whitish crystals; yield: 94%; mp: 277–9 °C dec. (ethanol). ^{1}H NMR (300 MHz, DMSO-d_6) δ: 4.67 (s, 2H), 5.23 (s, 2H), 5.65 (s, 1H), 7.00–7.07 (m, 2H), 7.33–7.38 (m, 1H), 7.42–7.48 (m, 1H), 7.52–7.55 (m, 2H), 7.68 (s, 2H, dis. with D_2O), 7.98 (d, J = 8.8 Hz, 1H). Anal. ($C_{18}H_{14}BrNO_5$) C, H, N.

*8.1.6.2. 2-({7-[(3-Chlorobenzyl)oxy]-2-oxo-2H-chromen-4-yl}oxy) acetamide (**6b**).* Whitish crystals; yield: 80%; mp: 283–4 °C dec. (acetone). ^{1}H NMR (200 MHz, DMSO-d_6) δ: 4.71 (s, 2H), 5.27 (s, 2H), 5.68 (s, 1H), 6.95–7.15 (m, 2H), 7.33–7.51 (m, 3H), 7.58 (s, 1H), 7.73 (s, 2H, dis. with D_2O), 8.00 (d, J = 8.8 Hz, 1H). Anal. ($C_{18}H_{14}ClNO_5$) C, H, N.

*8.1.6.3. 2-({7-[(3-Chlorobenzyl)oxy]-2-oxo-2H-chromen-4-yl}oxy)-N-methylacetamide (**6c**).* Obtained by the reaction of acyl chloride of **5a** with methylamine. White crystals; yield: 94%; mp: 193–5 °C (CH_2Cl_2/ethyl acetate). ^{1}H NMR (200 MHz, DMSO-d_6) δ: 2.71 (d, J = 4.8 Hz, 3H), 4.74 (s, 2H), 5.27 (s, 2H), 5.71 (s, 1H), 7.01–7.16 (m, 2H), 7.37–7.55 (m, 3H), 7.58 (s, 1H), 8.02 (d, J = 8.8 Hz, 1H), 8.16 (br q, 1H, dis. with D_2O). Anal. ($C_{19}H_{16}ClNO_5$) C, H, N.

*8.1.6.4. 2-({7-[(3-Chlorobenzyl)oxy]-2-oxo-2H-chromen-4-yl}oxy)-N,N-dimethylacetamide (**6d**).* Obtained by the reaction of acyl chloride of **5a** with dimethylamine. White crystals; yield: 85%; mp: 152–3 °C (ethyl acetate). ^{1}H NMR (200 MHz, $CDCl_3$) δ: 3.05 (s, 3H), 3.09 (s, 3H), 4.87 (s, 2H), 5.12 (s, 2H), 5.53 (s, 1H), 6.86 (s, 1H), 6.93 (d, J = 8.8 Hz, 1H), 7.26–7.41 (m, 3H), 7.46 (s, 1H), 7.85 (d, J = 8.8 Hz, 1H). Anal. ($C_{20}H_{18}ClNO_5$) C, H, N.

*8.1.6.5. 7-[(3-Chlorobenzyl)oxy]-4-(2-oxo-2-piperidin-1-ylethoxy)-2H-chromen-2-one (**6e**).* Obtained by the reaction of acyl chloride of **5a** with piperidine. White crystals; yield: 72%; mp: 146–7 °C (ethyl acetate). ^{1}H NMR (200 MHz, $CDCl_3$) δ: 1.47–1.78 (m, 6H), 3.32–3.70 (m, 4H), 4.87 (s, 2H), 5.12 (s, 2H), 5.55 (s, 1H), 6.85 (d, J = 2.4 Hz, 1H), 6.93 (dd, J_1 = 2.4 Hz, J_2 = 8.8 Hz, 1H), 7.21–7.40 (m, 3H), 7.46 (s, 1H), 7.83 (d, J = 8.8 Hz, 1H). Anal. ($C_{23}H_{22}ClNO_5$) C, H, N.

*8.1.6.6. 7-[(3-Chlorobenzyl)oxy]-4-(2-morpholin-4-yl-2-oxoethoxy)-2H-chromen-2-one (**6f**).* Obtained by the reaction of acyl chloride of **5a** with morpholine. White crystals; yield: 79%; mp: 161–3 °C (ethyl acetate/petroleum ether). ^{1}H NMR (200 MHz, $CDCl_3$) δ: 3.42–3.90 (m, 8H), 4.89 (s, 2H), 5.12 (s, 2H), 5.58 (s, 1H), 6.86 (d, J = 2.4 Hz, 1H), 6.94 (dd, J_1 = 2.4 Hz, J_2 = 8.8 Hz, 1H), 7.21–7.40 (m, 3H), 7.46 (s, 1H), 7.80 (d, J = 8.8 Hz, 1H). Anal. ($C_{22}H_{20}ClNO_6$) C, H, N.

*8.1.7. ({7-[(3-Chlorobenzyl)oxy]-2-oxo-2H-chromen-4-yl}oxy) acetonitrile (**7**)*

Amide **6b** (0.36 g, 1.0 mmol) was suspended in $POCl_3$ (10 mL) and the mixture was refluxed for 2 h, with stirring. The resulting solution was poured into ice-water and, after hydrolysis of excess $POCl_3$, was exhaustively extracted with CH_2Cl_2. The combined extracts were dried over anhydrous Na_2SO_4 and concentrated in vacuo. Chromatographic separation on a silica gel column, by eluting with the mixture CH_2Cl_2/ethyl acetate (1:1, v/v) gave pure compound **7**. White crystals; yield: 61%; mp: 157–8 °C (ethyl acetate). ^{1}H NMR (200 MHz, $CDCl_3$) δ: 4.96 (s, 2H), 5.14 (s, 2H), 5.69 (s, 1H), 6.89 (d, J = 2.4 Hz, 1H), 6.97 (dd, J_1 = 2.4 Hz, J_2 = 8.8 Hz, 1H), 7.25–7.40 (m, 3H), 7.46 (s, 1H), 7.73 (d, J = 8.8 Hz, 1H). Anal. ($C_{18}H_{12}ClNO_4$) C, H, N.

*8.1.8. 4-Chloro-7-[(3-chlorobenzyl)oxy]-2H-chromen-2-one (**8**)*

Triethylamine (5 mL) was added to 7-[(3-chlorobenzyl)oxy]-4-hydroxycoumarin **2c** (0.91 g, 3.0 mmol) previously suspended in methanol (5 mL). The resulting solution was evaporated to dryness in vacuo to give a resinous residue to which $POCl_3$ (5 mL) was added. The mixture was heated at 130 °C for 3 h, with stirring. The dark solution obtained was poured into ice-water and, after hydrolysis of excess $POCl_3$, was exhaustively extracted with CH_2Cl_2.

The combined extracts were dried over anhydrous Na_2SO_4, concentrated in vacuo, and chromatographed on a silica gel column, eluting with CH_2Cl_2 to give pure compound **8**. White crystals; yield: 66%; mp: 175–7 °C (ethyl acetate). ^{1}H NMR (200 MHz, $CDCl_3$) δ: 5.15 (s, 2H), 6.48 (s, 1H), 6.90 (d, J = 2.4 Hz, 1H), 7.01 (dd, J_1 = 2.4 Hz, J_2 = 8.8 Hz, 1H), 7.23–7.40 (m, 3H), 7.46 (s, 1H), 7.80 (d, J = 8.8 Hz, 1H). Anal. ($C_{16}H_{10}Cl_2O_3$) C, H.

*8.1.9. 7-[(3-Chlorobenzyl)oxy]-4-phenoxy-2H-chromen-2-one (**9**)*

The mixture of 4-chlorocoumarin **8** (0.32 g, 1.0 mmol), phenol (1.9 g, 20 mmol), anhydrous K_2CO_3 (1.0 g, 7.2 mmol) and 2-butanone (40 mL) was refluxed for 2 h with stirring. The solvent was then removed in vacuo and the residue was partitioned between H_2O and CH_2Cl_2. The organic layer was collected and the aqueous phase was further extracted twice with CH_2Cl_2. The combined extracts were washed with 0.5 N aqueous NaOH (to remove the excess phenol), then with water and dried over Na_2SO_4. After removal of solvent, pure compound **9** was obtained. White crystals; yield: 74%; mp: 164–5 °C (ethyl acetate/petroleum ether). ^{1}H NMR (200 MHz, $CDCl_3$) δ: 5.16 (s, 2H), 5.31 (s, 1H), 6.91 (d, J = 2.4 Hz, 1H), 7.03 (dd, J_1 = 2.4 Hz, J_2 = 8.8 Hz, 1H), 7.10–7.60 (m, 9H), 7.96 (d, J = 8.8 Hz, 1H). Anal. ($C_{22}H_{15}ClO_4$) C, H.

*8.1.10. 4-Amino-7-[(3-chlorobenzyl)oxy]-2H-chromen-2-one (**10a**)*

The mixture of 4-hydroxycoumarin **2c** (1.2 g, 4.0 mmol), ammonium acetate (2.0 g, 26 mmol) and DMSO (10 mL) was heated at 120 °C for 3 h, with stirring. The resulting solution was poured into cold water (~300 mL) and the amorphous solid that separated out was recovered by filtration, washed with water and dried. This solid (mixture of starting compound **2c** and 4-aminoderivative **10a**) was finely powdered in a mortar, then stirred in hot CH_2Cl_2 for 15 min. The resulting suspension was filtered to give a good recovery (0.30 g) of starting compound **2c**. The filtrate was concentrated in vacuo, then purified through a silica gel column, eluting with the mixture CH_2Cl_2/ethyl acetate (1:1, v/v). The eluate collected afforded pure compound **10a**. White crystals; yield: 48%; mp: 248–250 °C (ethanol). ^{1}H NMR (200 MHz, DMSO-d_6) δ: 5.09 (s, 1H), 5.24 (s, 2H), 6.88–7.08 (m, 2H), 7.23–7.52 (m, 5H, 2 protons dis. with D_2O), 7.57 (s, 1H), 7.92 (d, J = 8.8 Hz, 1H). Anal. ($C_{16}H_{12}ClNO_3$) C, H, N.

*8.1.11. N-{7-[(3-Chlorobenzyl)oxy]-2-oxo-2H-chromen-4-yl} acetamide (**10b**)*

In a closed Pyrex vessel equipped with a magnetic stirring bar, **10a** (0.30 mmol, 0.091 g) was suspended in acetic anhydride (2.0 mL). The reaction was exposed to microwave irradiation (150 °C, 30 min), cooled to room temperature and poured into crushed ice. The resulting precipitate was filtered, thus yielding the desired product that was further purified by crystallization from hot ethanol. White crystals; yield: 85%; mp: 139–141 °C dec. (ethanol). ^{1}H NMR (300 MHz, DMSO-d_6) δ: 2.31 (s, 3H), 5.25 (s, 2H), 6.61 (s, 1H), 7.01 (dd, J_1 = 1.7 Hz, J_2 = 8.8 Hz, 1H), 7.07 (d, J = 8.8 Hz, 1H), 7.19 (d, J = 1.7 Hz, 1H), 7.41–7.43 (m, 3H), 7.55 (s, 1H), 9.95 (br s, 1H, dis. with D_2O). Anal. ($C_{18}H_{14}ClNO_4$) C, H, N.

*8.1.12. Ethyl {7-[(3-chlorobenzyl)oxy]-2-oxo-2H-chromen-4-yl} carbamate (**10c**)*

Compound **10a** (0.30 mmol, 0.091 g) and anhydrous potassium carbonate (0.30 mmol, 0.041 g) were refluxed for 10 h under magnetic stirring in 2.0 mL of ethyl chloroformate. The reaction was cooled at room temperature, poured into crushed ice and filtered. The precipitate was purified on column chromatography (ethyl acetate/*n*-hexane 2:1 v/v as eluent). White crystals; yield: 46%. ^{1}H NMR (300 MHz, $CDCl_3$) δ: 1.41 (t, J = 7.2 Hz, 3H), 4.40 (q, J = 7.2 Hz, 2H), 5.11 (s, 2H), 6.50 (s, 1H), 6.88 (d, J = 2.4 Hz, 1H), 6.94 (dd, J_1 = 2.4 Hz, J_2 = 8.7 Hz, 1H), 6.98 (br s, 1H, dis. with D_2O), 7.28–7.37 (m, 3H), 7.43 (s, 1H), 7.65 (d, J = 8.7 Hz, 1H). Anal. ($C_{19}H_{16}ClNO_5$) C, H, N.

*8.1.13. N-{7-[(3-Chlorobenzyl)oxy]-2-oxo-2H-chromen-4-yl}-N′-ethylurea (**10d**)*

In a closed Pyrex vial equipped with a magnetic stirring bar, **10a** (0.30 mmol, 0.091 g) was suspended in ethyl isocyanate (2.0 mL). The vessel was kept for 5 days in an oil bath at 60 °C, then cooled at room temperature and the mixture poured into crushed ice. The resulting precipitate was filtered and crystallized from ethanol. White crystals; yield: 84%; mp: 227–8 °C (ethanol). ^{1}H NMR (300 MHz, DMSO-d_6) δ: 1.16 (t, J = 6.9 Hz, 3H), 3.81 (q, J = 6.9 Hz, 2H), 5.26 (s, 2H), 6.63 (s, 1H), 7.03 (dd, J_1 = 2.4 Hz, J_2 = 9.0 Hz, 1H), 7.19 (d, J = 2.4 Hz, 1H), 7.41–7.43 (m, 3H), 7.55 (s, 1H), 7.88 (d, J = 9.0 Hz, 1H), 2 NH not detected. Anal. ($C_{19}H_{17}ClN_2O_4$) C, H, N.

*8.1.14. 7-[(3-Chlorobenzyl)oxy]-4-(methylamino)-2H-chromen-2-one (**11a**)*

4-Chlorocoumarin derivative **8** (0.24 g, 0.75 mmol) was suspended in a solution of methylamine 60% wt. in ethanol (8.0 mL) and heated at 60 °C in a closed Pyrex vessel for 7 h, with stirring. After cooling at room temperature, the solvent and the excess amine were removed under reduced pressure and the resulting crude solid was purified through flash chromatography (gradient eluent, ethyl acetate in *n*-hexane 40% → 100%) to give pure compound **11a**. White crystals; yield: 46%; mp: 205–7 °C (diethyl ether). ^{1}H NMR (300 MHz, DMSO-d_6) δ: 2.81 (d, J = 4.7 Hz, 3H), 4.94 (s, 1H), 5.20 (s, 2H), 6.95 (d, J = 2.5 Hz, 1H), 6.99 (dd, J_1 = 2.5 Hz, J_2 = 8.8 Hz, 1H), 7.39–7.42 (m, 3H), 7.53 (s, 1H), 7.68 (br q, J = 4.7 Hz, 1H, dis. with D_2O). 7.86 (d, J = 8.8 Hz, 1H). Anal. ($C_{17}H_{14}ClNO_3$) C, H, N.

*8.1.15. 7-[(3-Chlorobenzyl)oxy]-4-(ethylamino)-2H-chromen-2-one (**11b**)*

The mixture of 4-chlorocoumarin derivative **8** (0.24 g, 0.75 mmol), ethylamine hydrochloride (0.61 g, 7.5 mmol) and triethylamine (2.0 mL) in ethanol (25 mL) was refluxed for 2 h, with stirring. The mixture was then evaporated to dryness in vacuo and the residue was partitioned between aqueous 5% $NaHCO_3$ and CH_2Cl_2. The organic layer was collected and the aqueous phase was further extracted twice with CH_2Cl_2. The combined extracts were dried over anhydrous Na_2SO_4, concentrated in vacuo, and chromatographed on a silica gel column, eluting with the mixture CH_2Cl_2/ethyl acetate (1:1, v/v) to give pure compound **11b**. White crystals; yield: 73%; mp: 183–4 °C (ethyl acetate/petroleum ether). ^{1}H NMR (200 MHz, $CDCl_3$) δ: 1.39 (t, J = 7.2 Hz, 3H), 1.80–2.30 (br s, 1H, dis. with D_2O), 3.34 (q, J = 7.2 Hz, 2H), 5.11 (s, 2H), 5.25 (s, 1H), 6.80–6.97 (m, 2H), 7.24–7.55 (m, 5H). Anal. ($C_{18}H_{16}ClNO_3$) C, H, N.

*8.1.16. 7-[(3-Chlorobenzyl)oxy]-4-(isopropylamino)-2H-chromen-2-one (**11c**)*

The mixture of 4-chlorocoumarin derivative **8** (0.24 g, 0.75 mmol), isopropylamine (3.0 mL) and CH_2Cl_2 (25 mL) was refluxed for 5 h, with stirring. The mixture was then diluted with CH_2Cl_2, transferred in a separatory funnel and washed with aqueous 5% $NaHCO_3$. The organic solution was collected, dried over anhydrous Na_2SO_4, and evaporated to dryness in vacuo to give an oily residue which was chromatographed on a silica gel column, eluting first with CH_2Cl_2 to remove some impurities, then with the mixture CH_2Cl_2/ethyl acetate (1:1, v/v). The eluate collected afforded pure compound **11c**. White crystals; yield: 47%; mp: 180–2 °C (ethyl acetate/petroleum ether). ^{1}H NMR (300 MHz, DMSO-d_6) δ: 1.21 (d, J = 6.1 Hz, 6H), 3.76 (m, 1H), 5.02 (s, 1H), 5.20 (s, 2H), 6.93–6.99 (m, 2H), 7.13 (d, J = 7.4 Hz, 1H, dis. with D_2O), 7.39–7.43 (m, 3H), 7.53 (s, 1H), 8.05 (d, J = 8.8 Hz, 1H). Anal. ($C_{19}H_{18}ClNO_3$) C, H, N.

*8.1.17. 4-Anilino-7-[(3-chlorobenzyl)oxy]-2H-chromen-2-one (**11d**)*

4-Chlorocoumarin derivative **8** (0.096 g, 0.30 mmol) was suspended in aniline (1.0 mL) and *N*,*N*-diisopropylethylamine (0.11 mL, 0.60 mmol) was added. The mixture was heated at 140 °C for 48 h and then partitioned between brine (50 mL) and diethyl ether (30 mL). The organic layer was washed with brine (3 × 20 mL) and then dried over Na_2SO_4. After removal of the solvent under vacuum, the mixture was purified by flash chromatography (gradient eluent, methanol in dichloromethane 0% → 5%) yielding the desired product **11d**. Brown powder; yield: 53%, mp: 221–3 °C. ^{1}H NMR (300 MHz, DMSO-d_6) δ: 5.16 (s, 1H), 5.25 (s, 2H), 7.03 (d, J = 2.5 Hz, 1H), 7.08 (dd, J_1 = 2.5 Hz, J_2 = 8.8 Hz, 1H), 7.27 (t, J = 7.7 Hz, 1H), 7.34 (d, J = 7.7 Hz, 2H), 7.41–7.49 (m, 5H), 7.55 (s, 1H), 8.15 (d, J = 8.8 Hz, 1H), 9.23 (s, 1H, dis. with D_2O). Anal. ($C_{22}H_{16}ClNO_3$) C, H, N.

*8.1.18. **7**-[(3-Chlorobenzyl)oxy]-4-ethyl-2H-chromen-2-one (**13b**)*

Intermediate **12b** [42] (1.9 g, 10 mmol) was added to an ethanol solution of sodium ethoxide (10 mmol, 0.23 g of sodium) and the resulting solution was evaporated to dryness in vacuo. To the solid residue DMF (30 mL) and 3-chlorobenzyl chloride (1.6 g, 10 mmol) were added and the mixture was heated at 100 °C for 1 h with stirring. The resulting solution was poured into cold water (400 mL) so that the nearly pure compound **13b** separated out as a whitish solid that was recovered by filtration, washed with water and dried. White solid; yield: 83%; mp: 130–1 °C (ethyl acetate/petroleum ether). ^{1}H NMR (300 MHz, $CDCl_3$) δ: 1.32 (t, J = 7.4 Hz, 3H), 2.78 (q, J = 7.4 Hz, 2H), 5.10 (s, 2H), 6.16 (s, 1H), 6.87 (d, J = 2.5 Hz, 1H), 6.93 (dd, J_1 = 2.5 Hz, J_2 = 8.8 Hz, 1H), 7.28–7.35 (m, 3H), 7.44 (s, 1H), 7.55 (d, J = 8.8 Hz, 1H). Anal. ($C_{18}H_{15}ClO_3$) C, H.

*8.1.19. 7-[(3-Chlorobenzyl)oxy]-4-(chloromethyl)-2H-chromen-2-one (**13c**)*

4-Chloromethylcoumarin **12c** (2.1 g, 10 mmol) was dissolved in dry DMF (35 mL) and then Cs_2CO_3 (3.9 g, 12 mmol) was added followed by 3-chlorobenzyl bromide (1.3 mL, 10 mmol) after 15 min of stirring. The mixture was stirred at room temperature for 24 h and then poured onto crushed ice. The resulting solid was filtered, washed several times with hot water and crystallized from $CHCl_3$/*n*-hexane yielding the desired product. Yield: 87%. Spectroscopic and analytical data are in full agreement with those reported in the literature [39].

*8.1.20. 7-[(3-Chlorobenzyl)oxy]-4-(hydroxymethyl)-2H-chromen-2-one (**13d**)*

7-Hydroxy-4-(hydroxymethyl)-2*H*-chromen-2-one **12d** [43] (0.38 g, 2.0 mmol) was dissolved in dry DMF (8.0 mL) followed by the addition of Cs_2CO_3 (0.65 g, 2.0 mmol). After stirring for 30 min, 3-chlorobenzyl bromide (0.64 mL, 2.0 mmol) was added. The resulting mixture was stirred at room temperature for 48 h and the solvent was evaporated under reduced pressure. The resulting solid was partitioned between brine (80 mL) and chloroform. After extraction with chloroform (3 × 40 mL), the organic phases were collected, dried over Na_2SO_4 and concentrated under vacuum. Crystallization of the obtained crude yellow solid from ethyl acetate furnished the desired compound. Yellow crystals; yield: 64%; mp: 185–6 °C (ethyl acetate). ^{1}H NMR (300 MHz, DMSO-d_6) δ: 4.71 (d, J = 3.3 Hz, 2H), 5.23 (s, 2H), 5.59 (t, J = 3.3 Hz, 1H, dis. with D_2O), 6.29 (s, 1H), 7.00 (dd, J_1 = 2.6 Hz, J_2 = 8.8 Hz, 1H), 7.07 (d, J = 2.6 Hz, 1H), 7.35–7.43 (m, 3H), 7.53 (s, 1H), 7.61 (d, J = 8.8 Hz, 1H). Anal. ($C_{17}H_{13}ClO_4$) C, H.

*8.1.21. General procedure for the synthesis of amino-compounds **13h–k***

Coumarin **13c** (0.17 g, 0.50 mmol) was dissolved in THF (5.0 mL) and the suitable amine (*n*-propylamine for **13h**: 0.82 mL, 10 mmol; *n*-butylamine for **13i**: 0.98 mL, 10 mmol; pyrrolidine for **13j**: 0.25 mL, 3.0 mmol; morpholine for **13k**: 0.26 mL, 3.0 mmol) was added. The reaction mixture was stirred at room temperature under an Argon atmosphere for 3 h. The excess amine and the solvent were removed under reduced pressure. The resulting crude oil was purified by flash chromatography (gradient eluent, ethyl acetate in *n*-hexane 40% → 100% for **13h–i** or ethyl acetate in *n*-hexane 0% → 50% for **13j–k**) yielding the desired compounds. The isolated free amines **13h–i**, corresponding to the fluorescent TLC spots with lower R_f, were transformed in the corresponding hydrochloride salts by using a commercially available 4.0 N solution of HCl in 1,4-dioxane.

*8.1.21.1. 7-[(3-Chlorobenzyl)oxy]-4-[(propylamino)methyl]-2H-chromen-2-one hydrochloride (**13h**).* White solid; yield: 59%; mp: 241–3 °C. ^{1}H NMR (300 MHz, DMSO-d_6) δ: 0.92 (t, J = 7.4 Hz, 3H), 1.69 (sext, J = 7.4 Hz, 2H), 2.99 (t, J = 7.4 Hz, 2H), 4.42 (s, 2H), 5.27 (s, 2H), 6.51 (s, 1H), 7.11 (dd, J_1 = 2.4 Hz, J_2 = 9.1 Hz, 1H), 7.15 (d, J = 2.5 Hz, 1H), 7.40–7.44 (m, 3H), 7.54 (s, 1H), 7.78 (d, J = 9.1 Hz, 1H), 9.06 (br s, 2H, dis. with D_2O). Anal. ($C_{20}H_{20}ClNO_3 \cdot HCl$) C, H, N.

*8.1.21.2. 4-[(Butylamino)methyl]-7-[(3-chlorobenzyl)oxy]-2H-chromen-2-one hydrochloride (**13i**).* White solid; yield: 43%; mp: 217.6–219.4 °C. ^{1}H NMR (300 MHz, DMSO-d_6) δ: 0.90 (t, J = 7.2 Hz, 3H), 1.35 (sext, J = 7.2 Hz, 2H), 1.64 (quint, J = 7.2 Hz, 2H), 3.03 (t, J = 7.2 Hz, 2H), 4.42 (s, 2H), 5.27 (s, 2H), 6.50 (s, 1H), 7.10–7.15 (m, 2H), 7.39–7.45 (m, 3H), 7.54 (s, 1H), 7.78 (d, J = 8.8 Hz, 1H), 9.02 (br s, 2H, dis. with D_2O) Anal. ($C_{21}H_{22}ClNO_3 \cdot HCl$) C, H, N.

*8.1.21.3. 7-[(3-Chlorobenzyl)oxy]-4-(pyrrolidin-1-ylmethyl)-2H-chromen-2-one (**13j**).* White solid; yield: 79%; mp: 120–121.7 °C. ^{1}H NMR (300 MHz, DMSO-d_6) δ: 1.68–1.72 (m, 4H), 2.50–2.52 (m, 4H), 3.74 (s, 2H), 5.23 (s, 2H), 6.28 (s, 1H), 7.01 (dd, J_1 = 2.5 Hz, J_2 = 8.8 Hz, 1H), 7.06 (d, J = 2.5 Hz, 1H), 7.39–7.44 (m, 3H), 7.53 (s, 1H), 7.83 (d, J = 8.8 Hz, 1H). Anal. ($C_{21}H_{20}ClNO_3$) C, H, N.

*8.1.21.4. 7-[(3-Chlorobenzyl)oxy]-4-(morpholin-4-ylmethyl)-2H-chromen-2-one (**13k**).* White solid; yield: 88%; mp: 140.8–142.6. ^{1}H NMR (300 MHz, DMSO-d_6) δ: 2.43–2.46 (m, 4H), 3.55–3.58 (m, 4H), 3.63 (s, 2H), 5.23 (s, 2H), 6.31 (s, 1H), 7.02 (dd, J_1 = 2.5 Hz, J_2 = 8.8 Hz, 1H), 7.06 (d, J = 2.5 Hz, 1H), 7.37–7.44 (m, 3H), 7.53 (s, 1H), 7.86 (d, J = 8.8 Hz, 1H). Anal. ($C_{21}H_{20}ClNO_4$) C, H, N.

*8.1.22. 7-[(3-Bromobenzyl)oxy]-4-(chloromethyl)-2H-chromen-2-one (**13l**)*

4-Chloromethylcoumarin **12c** (0.42 g, 2.0 mmol) was dissolved in dry DMF (10 mL) and then Cs_2CO_3 (0.65 g, 2.0 mmol) was added followed by 3-bromobenzyl bromide (0.75 g, 3.0 mmol) after 15 min of stirring. Stirring was continued at room temperature for 24 h and then reaction mixture was poured onto crushed ice. After extraction with ethyl acetate (3 × 120 mL), the organic phases were collected, dried over Na_2SO_4 and concentrated under vacuum. Flash chromatographic separation (gradient eluent, ethyl acetate in *n*-hexane 0% → 50%) afforded pure **13l**. Whitish crystals; yield: 61%; mp: 126.5–128 °C (diethyl ether). ^{1}H NMR (300 MHz, DMSO-d_6) δ: 4.98 (s, 2H), 5.24 (s, 2H), 6.49 (s, 1H), 7.09 (dd, J_1 = 2.5 Hz, J_2 = 8.8 Hz, 1H), 7.12 (d, J = 2.5 Hz, 1H), 7.34–7.39 (m, 1H), 7.46–7.48 (m, 1H), 7.53–7.55 (m, 1H), 7.68 (s, 1H), 7.77 (d, J = 8.8 Hz, 1H). Anal ($C_{17}H_{12}BrClO_3$) C, H.

*8.1.23. 7-[(3-Bromobenzyl)oxy]-4-(hydroxymethyl)-2H-chromen-2-one (**13m**)*

4-Chloromethylcoumarin **13l** (0.11 g, 0.30 mmol) was refluxed in water (50 mL) for 48 h. After cooling at room temperature, the reaction mixture was extracted with chloroform (3 × 20 mL). The organic layers were collected, dried over Na_2SO_4 and concentrated to dryness. The resulting crude solid was purified by flash

chromatography, thus obtaining the desired alcohol **13m**. White solid; yield: 46%; mp: 184.8–186.2 °C (diethyl ether). ^{1}H NMR (300 MHz, DMSO-d_6) δ: 4.71 (d, J = 5.5 Hz, 2H), 5.23 (s, 2H), 5.60 (t, J = 5.5 Hz, 1H, dis. with D_2O), 6.29 (s, 1H), 6.98–7.03 (m, 1H), 7.08–7.09 (m, 1H), 7.33–7.39 (m, 1H), 7.45–7.48 (m, 1H), 7.52–7.55 (m, 1H), 7.61 (d, J = 9.1 Hz, 1H), 7.67 (s, 1H). Anal ($C_{17}H_{13}BrO_4$) C, H.

8.1.24. 7-[(3-Bromobenzyl)oxy]-4-[(methylamino)methyl]-2H-chromen-2-one hydrochloride (**13n**)

4-Chloromethylcoumarin **13l** (0.11 g, 0.30 mmol) was dissolved in THF (1.0 mL) and the commercially available 2.0 N solution of methylamine in THF (3.0 mL, 6.0 mmol) was added. The reaction mixture was stirred at room temperature for 3 h. After the removal of the excess amine and the solvent under reduced pressure, the resulting crude oil was purified by flash chromatography (gradient eluent, ethyl acetate in *n*-hexane 40% → 100%) and the isolated free amine, corresponding to the fluorescent TLC spots with lower R_f, was transformed in the corresponding hydrochloride salts by using a commercially available HCl 4.0 N solution in 1,4-dioxane. White solid; yield: 66%; mp: 236–7 °C. ^{1}H NMR (300 MHz, DMSO-d_6) δ: 2.68 (s, 3H), 4.42 (s, 2H), 5.26 (s, 2H), 6.46 (s, 1H), 7.10 (dd, J_1 = 2.5 Hz, J_2 = 8.8 Hz, 1H), 7.15 (d, J = 2.5 Hz, 1H), 7.34–7.39 (m, 1H), 7.46–7.48 (m, 1H), 7.53–7.55 (m, 1H), 7.68 (s, 1H), 7.77 (d, J = 8.8 Hz, 1H), 9.30 (br s, 2H, dis. with D_2O). Anal. ($C_{18}H_{16}BrNO_3 \cdot HCl$) C, H, N.

8.1.25. 7-[(3-Chlorobenzyl)oxy]-4-(1-hydroxyethyl)-2H-chromen-2-one (**14**)

The mixture of **13b** (1.3 g, 4.0 mmol) and selenium dioxide (0.67 g, 6.0 mmol) in xylene (30 mL) was heated at 140 °C for 4 h, with stirring. The mixture was filtered to remove black selenium, and the filtrate was evaporated to dryness. The residue was dissolved in dichloromethane and chromatographed on a silica gel column eluting with the same solvent to remove a mixture of starting compound and 4-acetyl derivative by-product. The elution was then pursued with the mixture dichloromethane–ethyl acetate (1:1, v/v). The fraction collected, after removal of solvents, afforded an oily residue, from which, after the addition of a small volume diethyl ether, pure racemic compound **14** separated out as whitish crystals. Yield: 43%; mp: 111–2 °C (diisopropyl ether). ^{1}H NMR (300 MHz, DMSO-d_6) δ: 1.37 (t, J = 6.6 Hz, 3H), 5.07 (m, 1H), 5.23 (s, 2H), 5.58 (d, J = 4.4 Hz, 1H. dis. with D_2O), 6.31 (s, 1H), 7.02 (dd, J_1 = 2.5 Hz, J_2 = 8.8 Hz, 1H), 7.09 (d, J = 2.5 Hz, 1H), 7.41–7.44 (m, 3H), 7.54 (s, 1H), 7.79 (d, J = 8.8 Hz, 1H). Anal. ($C_{18}H_{15}ClO_4$) C, H.

8.1.26. 4-Acetyl-7-[(3-chlorobenzyl)oxy]-2H-chromen-2-one (**15**)

A suspension of pyridinium chlorochromate (0.49 g, 2.3 mmol) in 30 mL of CH_2Cl_2 was slowly added to a solution of **14** (0.50 g, 1.5 mmol) in CH_2Cl_2 (30 mL). This mixture was stirred at room temperature for 2 h, then filtered to remove a dark amorphous solid which was washed with dichloromethane and discarded. The organic phase was washed with abundant water in a separatory funnel to remove the inorganic impurities, then dried over Na_2SO_4 and evaporated to dryness in vacuo. The residue was dissolved in CH_2Cl_2 and chromatographed on a silica gel column eluting with the same solvent; the eluate collected, after removal of solvent, afforded pure compound **15**. Yellow crystals; yield: 46%; mp: 155–6 °C (diisopropyl ether). ^{1}H NMR (300 MHz, DMSO-d_6) δ: 2.61 (s, 3H), 5.24 (s, 2H), 6.82 (s, 1H), 7.04 (dd, J_1 = 2.5 Hz, J_2 = 8.8 Hz, 1H), 7.13 (d, J = 2.5 Hz, 1H), 7.39–7.43 (m, 3H), 7.53 (s, 1H), 7.77 (d, J = 8.8 Hz, 1H). Anal. ($C_{18}H_{13}ClO_4$) C, H.

8.1.27. 7-[(3-Chlorobenzyl)oxy]-2-oxo-2H-chromene-4-carbaldehyde (**16**)

Alcohol **13d** (0.38 g, 1.2 mmol) was suspended in dichloromethane (10 mL) and 4 Å powder molecular sieves (1.2 g) were added followed by sodium acetate (0.010 g, 0.12 mmol). While cooling at 0 °C, pyridinium chlorochromate (0.65 g, 3.0 mmol) was added in 3 portions. The mixture was slowly brought back to room temperature and then stirred for 12 h. The mixture was filtered over a silica pad and then washed with chloroform. The solution was concentrated under reduced pressure and the resulting solid was purified by flash chromatography. Pure aldehyde **16** was obtained as a yellow solid. Yield: 46%. Spectroscopic and analytic data are in agreement with those reported in the literature [43].

8.1.28. 7-[(3-Chlorobenzyl)oxy]-2-oxo-2H-chromene-4-carbaldehyde oxime (**17**)

According to a literature method [51], a mixture of hydroxylamine hydrochloride (0.076 g, 1.1 mol) and $AcONa \cdot 3H_2O$ (0.15 g, 1.1 mmol) previously dissolved in water (5 mL) was added to the solution of aldehyde **16** (0.31 g, 1.0 mmol) in hot ethanol (100 mL). The resulting mixture was refluxed for 30 min, then concentrated in vacuo and poured into cold water (300 mL). The nearly pure aldoxime **17** separated out as a whitish solid which was collected by filtration, washed with water and dried. Cream-coloured crystals; quantitative yield; mp: 232–5 °C (ethanol). ^{1}H NMR (300 MHz, DMSO-d_6) δ: 5.24 (s, 2H), 6.52 (s, 1H), 7.05–7.11 (m, 2H), 7.38–7.44 (m, 3H), 7.54 (s, 1H), 8.36 (d, J = 9.2 Hz, 1H), 8.41 (s, 1H), 12.35 (s, 1H, dis. with D_2O). Anal. ($C_{17}H_{12}ClNO_4$) C, H, N.

8.1.29. 7-[(3-Chlorobenzyl)oxy]-2-oxo-2H-chromene-4-carbonitrile (**18**)

Aldoxime **17** (0.26 g, 0.80 mmol) was suspended in acetic anhydride (10 mL) and the resulting mixture was then refluxed (140 °C) with stirring overnight. The resulting solution was evaporated to dryness in vacuo and the solid residue was partitioned between aqueous 5% $NaHCO_3$ (100 mL) and dichloromethane (100 mL); the aqueous phase was further extracted twice with dichloromethane. The combined extracts were dried over anhydrous Na_2SO_4 and evaporated to dryness, thus yielding the pure nitrile **18**. Whitish crystals; yield: 96%; mp: 180–1 °C (ethyl acetate/petroleum ether). ^{1}H NMR (300 MHz, DMSO-d_6) δ: 5.27 (s, 2H), 7.16 (dd, J_1 = 2.5 Hz, J_2 = 8.8 Hz, 1H), 7.19 (s, 1H), 7.21 (d, J = 2.5 Hz, 1H), 7.39–7.44 (m, 3H), 7.54 (s, 1H), 7.66 (d, J = 8.8 Hz, 1H). Anal. ($C_{17}H_{10}ClNO_3$) C, H, N.

8.1.30. Ethyl 7-[(3-chlorobenzyl)oxy]-2-oxo-2H-chromene-4-carboxylate (**20**)

Ester **19**[33] (0.46 g, 2.0 mmol) was dissolved in dry DMF (8 mL) and Cs_2CO_3 (0.65 g, 2.0 mmol) was added. The mixture turned from yellow to red in few minutes and then 3-chlorobenzyl bromide (0.32 mL, 2.4 mmol) was added. After stirring at room temperature for 24 h, the mixture was poured onto crushed ice and the resulting solid was filtered and washed with water. This precipitate was treated with a small volume of diethyl ether and the resulting solid was collected as the pure compound **20**. Off-white solid; yield: 93%; mp: 133.5–135.6 °C. ^{1}H NMR (300 MHz, DMSO-d_6) δ: 1.33 (t, J = 7.2 Hz, 3H), 4.35 (q, J = 7.2 Hz, 2H), 5.25 (s, 2H), 6.69 (s, 1H), 7.08 (dd, J_1 = 2.5 Hz, J_2 = 8.8 Hz, 1H), 7.15 (d, J = 2.5 Hz, 1H), 7.38–7.42 (m, 3H), 7.54 (s, 1H), 8.01 (d, J = 8.8 Hz, 1H). Anal. ($C_{19}H_{15}ClO_5$) C, H.

8.1.31. 7-[(3-Chlorobenzyl)oxy]-2-oxo-2H-chromene-4-carboxylic acid (**21**)

After complete dissolution of solid KOH (0.17 g, 3.0 mmol) in boiling ethanol (7.5 mL), ester **20** (0.54 g, 1.5 mmol) was added and the reflux was continued for 15 min. The mixture was slowly kept at room temperature and the solvent was evaporated under reduced pressure. The solid was diluted with water (50 mL) and the solution was made acid (pH ≈ 2) with 2.0 N HCl and then extracted with ethyl acetate (3 × 30 mL). The organic layers were collected dried

over Na_2SO_4 and concentrated to dryness yielding a yellow solid that was washed with diethyl ether furnishing acid **21**. Pale yellow solid; mp: 159–161 °C (dec.); yield: 89%. ^{1}H NMR (300 MHz, DMSO-d_6) δ: 5.24 (s, 2H), 6.64 (s, 1H), 7.07 (dd, $J_1 = 2.5$ Hz, $J_2 = 9.1$ Hz, 1H), 7.13 (d, $J = 2.5$ Hz, 1H), 7.39–7.44 (m, 3H), 7.54 (s, 1H), 8.08 (d, $J = 9.1$ Hz, 1H), OH not detected. Anal. ($C_{17}H_{11}ClO_5$) C, H.

*8.1.32. 7-[(3-Chlorobenzyl)oxy]-2-oxo-2H-chromene-4-carboxamide (**22**)*

Derivative **21** (0.33 g, 1.0 mmol) was suspended in dry CH_2Cl_2 (6 mL) and thionyl chloride (2.0 mL) was added. The reaction mixture was refluxed for 2 h and then evaporated to dryness. Concentrated aq. ammonia (5.0 mL) was added while cooling at 0 °C. The mixture was allowed to reach room temperature slowly and then stirred for 6 h. The excess ammonia and water were removed in vacuo. The resulting solid was washed several times with chloroform and filtered, giving pure amide **22**. An additional amount of product was obtained from chromatographic separation of the organic liquor (eluent, 5% methanol in chloroform, v/v). Brown solid; yield: 52%; mp: >230 °C. ^{1}H NMR (300 MHz, DMSO-d_6) δ: 5.24 (s, 2H), 6.36 (s, 1H), 7.05–7.08 (m, 1H), 7.11–7.13 (m, 1H), 7.38–7.42 (m, 3H), 7.54 (s, 1H), 7.72 (d, $J = 8.8$ Hz, 1H), 7.96 (s, 1H, dis. with D_2O), 8.26 (s, 1H, dis. with D_2O). Anal. ($C_{17}H_{12}ClNO_4$) C, H, N.

*8.1.33. 7-[(3-Chlorobenzyl)oxy]-2H-chromen-2-one (**23**)*

Commercial 7-hydroxycoumarin (0.16 g, 1.0 mmol) and 3-chlorobenzyl bromide (0.32 mL, 1.0 mmol) were reacted as described for **13d**. The workup rendered a crude that was purified by crystallization. White crystals; yield: 64%; mp: 127–8 °C (ethanol). ^{1}H NMR (300 MHz, $CDCl_3$) δ: 5.10 (s, 2H), 6.27 (d, $J = 9.6$ Hz, 1H), 6.87 (d, $J = 2.4$ Hz, 1H), 6.91 (dd, $J_1 = 2.4$ Hz, $J_2 = 8.4$ Hz, 1H), 7.32–7.34 (m, 3H), 7.39 (d, $J = 8.4$ Hz, 1H), 7.44 (s, 1H), 7.64 (d, $J = 9.6$ Hz, 1H). Anal. ($C_{16}H_{11}ClO_3$) C, H.

*8.1.34. 7-[(3-Chlorobenzyl)oxy]-4-(trifluoromethyl)-2H-chromen-2-one (**24**)*

Commercially available 7-hydroxy-4-trifluoromethyl coumarin (0.069 g, 0.30 mmol) was dissolved in dry DMF (2.0 mL) and then 60% NaH in mineral oil (0.012 g, 0.30 mmol) was added while cooling at 0 °C. The mixture was slowly warmed at room temperature, then 3-chlorobenzyl bromide (0.040 mL, 0.30 mmol) was added dropwise via syringe after 1 h and stirring was continued for 24 h at room temperature. After addition of crushed ice, the suspension was treated with 2.0 N aq. solution of NaOH (5 mL). The mixture was stirred for 1 h and the resulting precipitate was filtered and washed with water, yielding compound **24**. White crystals; yield: 84%, mp: 118.8–120.3 °C (ethanol). ^{1}H NMR (300 MHz, DMSO-d_6) δ: 5.27 (s, 2H), 6.85 (s, 1H), 7.13 (dd, $J_1 = 2.4$ Hz, $J_2 = 8.9$ Hz, 1H), 7.23 (d, $J = 2.4$ Hz, 1H), 7.40–7.45 (m, 3H), 7.54 (s, 1H), 7.61–7.64 (m, 1H). Anal. ($C_{17}H_{10}ClF_3O_3$) C, H.

8.2. Biological assays

MAO inhibitory activity of compounds in Table 1 was assessed using a continuous spectrophotometric assay, monitoring the rate of oxidation of the nonselective nonfluorescent MAO substrate kynuramine to 4-hydroxyquinoline. Briefly, male Sprague–Dawley rats (200–250 g) were sacrificed by decapitation. The brains were immediately removed and washed in an ice-cold isotonic Na_2HPO_4/KH_2PO_4 buffer (pH 7.40) containing sucrose. A crude brain mitochondrial fraction was then prepared by differential centrifugation [52] and stored at −40 °C in an isotonic Na_2HPO_4/KH_2PO_4 buffer (pH 7.4) containing KCl. MAO-A and MAO-B activities in mitochondrial preparations (1 mg/mL) were assayed using as selective and irreversible inhibitors clorgyline (250 nM) and (−)-L-deprenyl (250 nM), respectively. After a preincubation for 5 min with the assayed compound dissolved in DMSO at a final concentration of 5% (v/v), kynuramine was added at a concentration equal to the corresponding K_M value (90 μM for MAO-A and 60 μM for MAO-B). Then the rate of formation of 4-hydroxyquinoline was monitored at 314 nm for 5 min. Finally, IC_{50} values were determined by nonlinear regression of MAO inhibition vs − log of the concentration plots, using the program Origin, version 6.0 (Microcal Software Inc., Northampton, MA).

8.3. Computational methods

The coumarin inhibitors were built from the LigPrep module available in Maestro (vers. 9.2) starting from the reference inhibitor (entry 13, 4-FCBC), that is the 4-formyl-7-metachlorobenzyloxycoumarin, co-crystallized with hMAO-B (pdb code: 2v60). As already reported [39], the spatial model of the rMAO-B was constructed through homology modelling. According to a recent study of hMAO-B crystal structure, we designated as ordered eight water molecules labelled as w1055, w1159, w1166, w1171, w1206, w1224, w1309 and w1351 referring to the numbering reported in the cited hMAO-B X-ray complex.

8.3.1. Docking simulations

GOLD (vers. 5.1), a genetic algorithm-based software, was used for the docking study selecting GoldScore as a fitness function. GoldScore is made up of four components that account for protein-ligand binding energy: protein-ligand hydrogen bond energy (external H-bond), protein-ligand van der Waals energy (external vdw), ligand internal vdw energy (internal vdw), and ligand torsional strain energy (internal torsion). Parameters used in the fitness function (hydrogen bond energies, atom radii and polarizabilities, torsion potentials, hydrogen bond directionalities, and so forth) were taken from the GOLD parameter file. Docking runs on MAO-B enzyme were performed through GOLD program selecting GoldScore as a fitness function. For each coumarin inhibitor, 10 conformations were generated in a sphere of a 12 Å radius centred on phenolic oxygen atom of Y435. In our docking runs, the molecular scaffold of the best ranked solution of the 2v60 reference ligand docked into the rMAO-B was set as physical constraint to favour the occurrence of the known binding mode of *m*halogeno-7-benzyloxy substituents of coumarin inhibitors (together with a distance constraint between the backbone oxygen atom if Ile164 and halogen atom of the inhibitor). Docking simulations towards MAO-B were carried out by allowing torsions and flexibility to Q206 and Y398. As already reported [39], eight ordered water molecules were explicitly considered in all the docking runs.

Acknowledgements

The financial support from MIUR, Italy (Grant PRIN 20085HR5JK_005), is kindly acknowledged.

References

[1] M.B.H. Youdim, J.P.M. Finberg, K.F. Tipton, in: U. Trendelenburg, N. Weiner (Eds.), Catecholamine II. Handbook of Experimental Pharmacology, Springer, Berlin, 1988, pp. 127–199.
[2] D.E. Edmondson, A. Mattevi, C. Binda, M. Li, F. Hubálek, Curr. Med. Chem. 11 (2004) 1983–1993.
[3] J.P. Johnston, Biochem. Pharmacol. 17 (1968) 1285–1297.
[4] A.S. Kalgutkar, D.K. Dalvie, N. Castagnoli Jr., T.J. Taylor, Chem. Res. Toxicol. 14 (2001) 1139–1162.
[5] C. Binda, A. Mattevi, D.E. Edmondson, Int. Rev. Neurobiol. 100 (2011) 1–11.
[6] M. Li, F. Hubalek, P. Newton-Vinson, D.E. Edmondson, Protein Exp. Purif. 24 (2002) 152–162.

[7] P. Newton-Vinson, F. Hubalek, D.E. Edmondson, Protein Exp. Purif. 20 (2000) 334–345.
[8] I. Rebrin, R.M. Geha, K. Chen, J.C. Shih, J. Biol. Chem. 276 (2001) 29499–29506.
[9] C. Binda, M. Li, F. Hubalek, N. Restelli, D.E. Edmondson, A. Mattevi, Proc. Natl. Acad. Sci. U. S. A. 100 (2003) 9750–9755.
[10] F. Hubalek, C. Binda, A. Khalil, M. Li, A. Mattevi, N. Castagnoli, D.E. Edmondson, J. Biol. Chem. 280 (2005) 15761–15766.
[11] S.-Y. Son, Jichun Ma, Y. Kondou, M. Yoshimura, E. Yamashita, T. Tsukihara, Proc. Natl. Acad. Sci. U. S. A. 105 (2008) 5739–5744.
[12] L. De Colibus, M. Li, C. Binda, A. Lustig, D.E. Edmondson, A. Mattevi, Proc. Natl. Acad. Sci. U. S. A. 102 (2005) 12684–12689.
[13] C.H. Donnelly, D.L. Murphy, Biochem. Pharmacol. 26 (1977) 852–858.
[14] J.S. Fowler, R.R. MacGregor, A.P. Wolf, C.D. Arnett, S.L. Dewey, D. Schlyer, D. Christman, J. Logan, M. Smith, H. Sachs, Science 235 (1987) 481–485.
[15] J. Saura, R. Kettler, M. Da Prada, J.G. Richards, J. Neurosci. 12 (1992) 1977–1999.
[16] M.B. Youdim, D. Edmondson, K.F. Tipton, Nat. Rev. Neurosci. 7 (2006) 295–309.
[17] M.B.H. Youdim, Y.S. Bakhle, Br. J. Pharm. 147 (Suppl. 1) (2006) S287–S296.
[18] (a) M. Bortolato, K. Chen, J.C. Shih, Adv. Drug Deliv. Rev. 60 (2008) 1527–1533;
(b) G. Cohen, R. Farooqui, N. Kesler, Proc. Natl. Acad. Sci. U. S. A. 94 (1997) 4890–4894.
[19] J. Wouters, Curr. Med. Chem. 5 (1998) 137–162.
[20] J. Saura, E. Nadal, B. Van den Berg, M. Vila, J.A. Bombi, N. Mahy, Life Sci. 59 (1996) 1341–1349.
[21] M. Yamada, H. Yasuhara, Neurotoxicology 25 (2004) 215–221.
[22] J.D. Amsterdam, J. Clin. Psychiatry 64 (2003) 208–214.
[23] M.B. Youdim, A. Gross, J.P. Finberg, Br. J. Pharmacol. 132 (2001) 500–506.
[24] C.W. Olanow, O. Rascol, R. Hauser, New Engl. J. Med. 361 (2009) 1268–1278.
[25] N. Kaludercic, E. Takimoto, T. Nagayama, N. Feng, E.W. Lai, D. Bedja, K. Chen, K.L. Gabrielson, R.D. Blakely, J.C. Shih, K. Pacak, D.A. Kass, F. Di Lisa, N. Paolocci, Circ. Res. 106 (2010) 193–202.
[26] N. Kaludercic, A. Carpi, T. Nagayama, V. Sivakumaran, G. Zhu, E.W. Lai, D. Bedja, A. De Mario, K. Chen, K.L. Gabrielson, M.L. Lindsey, K. Pacak, E. Takimoto, J.C. Shih, D.A. Kass, F. Di Lisa, N. Paolocci, Antioxid. Redox Signal. (2013), http://dx.doi.org/10.1089/ars.2012.4616.
[27] M. Naoi, W. Maruyama, Curr. Pharm. Des. 16 (2010) 2799–2817.
[28] R. Morphy, Z. Rankovic, J. Med. Chem. 48 (2005) 6523–6543.
[29] M.B.H. Youdim, J.J. Buccafusco, Trends Pharmacol. Sci. 26 (2005) 27–35.
[30] L. Pisani, M. Catto, F. Leonetti, O. Nicolotti, A. Stefanachi, F. Campagna, A. Carotti, Curr. Med. Chem. 18 (2011) 4568–4587.
[31] A.M. Helguera, G. Perez-Machado, M.N. Cordeiro, F. Borges, Mini Rev. Med. Chem. 12 (2012) 907–919.
[32] M. Catto, O. Nicolotti, F. Leonetti, A. Carotti, A.D. Favia, R. Soto-Otero, E. Mendez-Alvarez, A. Carotti, J. Med. Chem. 49 (2006) 4912–4925.
[33] (a) L. Pisani, M. Barletta, R. Soto-Otero, O. Nicolotti, E. Mendez-Alvarez, M. Catto, A. Introcaso, A. Stefanachi, S. Cellamare, C. Altomare, A. Carotti, J. Med. Chem. 56 (2013) 2651–2664;
(b) O. Nicolotti, L. Pisani, M. Catto, F. Leonetti, I. Giangreco, A. Stefanachi, A. Carotti, Mol. Inform. 30 (2011) 133–136.
[34] F. Chimenti, D. Secci, A. Bolasco, P. Chimenti, B. Bizzarri, A. Granese, S. Carradori, M. Yáñez, F. Orallo, F. Ortuso, S. Alcaro, J. Med. Chem. 52 (2009) 1935–1942.
[35] F. Chimenti, A. Bolasco, D. Secci, B. Bizzarri, P. Chimenti, A. Granese, S. Carradori, J. Heterocycl. Chem. 47 (2010) 729–733.
[36] D. Viña, M.J. Matos, G. Ferino, E. Cadoni, R. Laguna, F. Borges, E. Uriarte, L. Santana, ChemMedChem 7 (2012) 464–470.
[37] M.J. Matos, C. Terán, Y. Pérez-Castillo, E. Uriarte, L. Santana, D. Viña, J. Med. Chem. 54 (2011) 7127–7137.
[38] C. Gnerre, M. Catto, F. Leonetti, P. Weber, P.-A. Carrupt, C. Altomare, A. Carotti, B. Testa, J. Med. Chem. 43 (2000) 4747–4758.
[39] L. Pisani, G. Muncipinto, T.F. Miscioscia, O. Nicolotti, F. Leonetti, M. Catto, C. Caccia, P. Salvati, R. Soto-Otero, E. Mendez-Alvarez, C. Passeleu, A. Carotti, J. Med. Chem. 52 (2009) 6685–6706.
[40] A. Carotti, P. Melloni, F. Thaler, C. Caccia, S. Maestroni, P. Salvati, WO 2006/102958 A1, 2006.
[41] (a) M. Di Braccio, G. Grossi, G. Roma, M.G. Signorello, G. Leoncini, Eur. J. Med. Chem. 39 (2004) 397–409;
(b) M.A. Hermodson, W.M. Barker, K.P. Link, J. Med. Chem. 14 (1971) 167–169.
[42] M.S. Manhas, S.N. Ganguly, S. Mukherjee, A.K. Jain, A.K. Bose, Tetrahedron Lett. 47 (2006) 2423–2425.
[43] C. Binda, J. Wang, L. Pisani, C. Caccia, A. Carotti, P. Salvati, D.E. Edmondson, A. Mattevi, J. Med. Chem. 50 (2007) 5848–5852.
[44] E. Mendez-Alvarez, R. Soto-Otero, I. Sanchez-Sellero, L.M. Lopez-Rivadulla, M. Lamas, Life Sci. 60 (1997) 1719–1727.
[45] C. Hansch, A. Leo, D. Hoekman, Exploring QSAR Hydrophobic, Electronic, and Steric Constants, in: ACS Professional Reference Book, vol. 2, American Chemical Society, Washington, DC, 1995.
[46] M.L. Verdonk, J.C. Cole, M.J. Hartshorn, C.W. Murray, R.D. Taylor, Proteins 52 (2003) 609–623.
[47] A. Carotti, C. Altomare, M. Catto, C. Gnerre, L. Summo, A. De Marco, S. Rose, P. Jenner, B. Testa, Chem. Biodivers. 3 (2006) 134–144.
[48] (a) C. Altomare, S. Cellamare, L. Summo, M. Catto, A. Carotti, U. Thull, P.-A. Carrupt, B. Testa, H. Stoeckly-Evans, J. Med. Chem. 41 (1998) 3812–3820;
(b) A. Carotti, M. Catto, F. Leonetti, F. Campagna, R. Soto-Otero, E. Méndez-Álvarez, U. Thull, B. Testa, C. Altomare, J. Med. Chem. 50 (2007) 5364–5372.
[49] A. Cavalli, M.L. Bolognesi, A. Minarini, M. Rosini, V. Tumiatti, M. Recanatini, C. Melchiorre, J. Med. Chem. 51 (2008) 347–372.
[50] (a) A. Carotti, MAOs long March: from toxic first-generation drugs to isoform-selective, reversible and multi-target inhibitors, in: Proceedings of the Meeting of ACS-EFMC, Frontiers in CNS and Oncology Medicinal Chemistry, Siena, Italy, October 7–9, 2007;
(b) A. Carotti, Multidisciplinary and multitarget approaches in the search for novel drugs in the treatment of neurodegenerative diseases, in: Proceedings of the XXIV National Meeting of the Italian Chemical Society Lecce, Italy, September 11–16, 2011.
[51] A.N. Brubaker, J. DeRuiter, W.L. Whitmer, J. Med. Chem. 29 (1986) 1094–1099.
[52] R. Soto-Otero, E. Mendez-Alvarez, A. Hermida-Ameijeiras, I. Sanchez-Sellero, A. Cruz-Landeira, M.L.R. Lamas, Life Sci. 69 (2001) 879–889.